

**MODELLING OF OPTICAL FIBRE SENSOR BASED ON
STIMULATED BRILLOUIN SCATTERING**

BY

KIRUI ESTHER CHERONO

**ATHESIS SUBMITTED IN PARTIAL FULFILLMENT OF THE
REQUIREMENTS FOR THE DEGREE OF MASTER OF SCIENCE IN
PHYSICS IN THE SCHOOL OF SCIENCE**

UNIVERSITY OF ELDORET, KENYA.

2014

DECLARATION

Declaration by the Candidate

This thesis is my own original work presented to University of Eldoret. The work has not been presented for a degree in any other university. No part of the research may be reproduced without prior knowledge of author and/or University of Eldoret.

Kirui Esther Cherono

SC/PGP/046/11

Signature.....Date.....

Declaration by the Supervisor

This thesis has been submitted for examinations with our approval as university supervisors.

Dr.David W.Waswa,

Department of Physics,

P.O. Box 1125, Eldoret.

Signature.....Date.....

Dr. Muguro Kennedy Mwaura,

Department of Physics,

P.O Box 1125, Eldoret.

Signature.....Date.....

DEDICATION

This research is dedicated to my family for their inspiration and unwavering support.

ABSTRACT

Distributed fibre optic sensing presents unique features that have no match in conventional sensing techniques. The ability to measure temperatures and strain at thousands of points along a single mode fibre is particularly interesting for monitoring of elongated structures such as pipelines, flow lines, oil wells and landslides. Brillouin Scattering in optical fibre is the result of the interaction between acoustic wave, a pump wave and a Stokes wave. In this research work investigations were carried out using VPI software for simulations. The probe wave was pulsed and launched into an optical fibre while the pump wave was launched through the other end of the fibre. The frequency difference between the two laser sources was set at 10.5-11GHz. This was used to investigate the existence of Stimulated Brillouin scattering in an optical fibre and the parameters affecting the backscattered power. The possibility of using these parameters to model a fibre optic sensor was done. Investigation showed that when the pump and Stokes (probe) wave counter propagate in the fibre there is transfer of energy between the pump and Stokes wave resulting in the pump and Stokes waves being depleted and amplified respectively as they travel along the fibre. Thus the Brillouin gain peaks at Brillouin frequency. Further investigations show that the backscattered power was low for input power below 5 dBm but increased rapidly above it and saturated above input power of 10 dBm for different fibre lengths. The effect of Polarization Mode Dispersion on Stimulated Brillouin scattering was found to decrease the signal power over time, this was due to differential group dispersion impairing the interaction between the pump and probe wave. Further results showed that power reduces with increase in temperature, the frequency shift (Brillouin shift) is directly proportional to temperature, and this was used to map out the temperature change along the fibre. The designed sensor can be used in civil structural monitoring of pipelines (i.e. leakage and intrusion), bridges, dams and railways for disaster prevention.

TABLE OF CONTENTS

DECLARATION	II
DEDICATION	III
ABSTRACT	IV
LIST OF FIGURES.....	VIII
LIST OF ABBREVIATIONS AND SYMBOLS.....	X
ACKNOWLEDGEMENT.....	XIII
CHAPTER ONE.....	1
INTRODUCTION	1
1.1 Background.....	1
1.2 PROBLEM STATEMENT.	3
1.3 JUSTIFICATION.....	3
1.4 OBJECTIVES.....	4
CHAPTER TWO.....	5
LITERATURE REVIEW.....	5
2.1 INTRODUCTION.....	5
2.2 ELECTRICAL SENSORS.....	5
2.3 OPTICAL FIBRES.....	6
2.4 FIBRE OPTIC SENSOR.....	7
2.5 TYPES OF FIBRE OPTIC SENSORS.....	8
2.5.1 Intensity-based Fibre Optic Sensor.....	9
2.5.2 Interferometric-based Fibre Optic Sensor.....	10
2.5.3 Polarization-based Fibre Optic Sensor(PFOS).....	12
2.6 THEORY OF BRILLOUIN SCATTERING.....	12
CHAPTER THREE.....	16
THEORY	16
3.1 INTRODUCTION.....	16
3.2 COUPLED-WAVE EQUATIONS.....	20
3.3 ELECTROSTRICTION.....	22
3.4 STIMULATED BRILLOUIN SCATTERING.....	24

3.5 STIMULATED BRILLOUIN THRESHOLD POWER.....	27
3.6 BRILLOUIN GAIN SPECTRUM	29
3.7 DISTRIBUTED OPTICAL FIBRE SENSOR BASED ON STIMULATED BRILLOUIN SCATTERING.....	30
3.8 SENSING PRINCIPLE	30
3.9 BRILLOUIN OPTICAL TIME DOMAIN ANALYSIS (BOTDA).....	31
3.10 BIREFRINGENCE.....	32
3.11 POLARIZATION MODE DISPERSION	34
3.12 POLARIZATION EFFECT ON THE BRILLOUIN FREQUENCY.....	36
CHAPTER FOUR	39
METHODOLOGY	39
4.1 INTRODUCTION	39
4.2 RESEARCH DESIGN	39
CHAPTER FIVE	42
RESULTS AND DISCUSSIONS	42
5.1 INTRODUCTION	42
5.2 EFFECT OF FREQUENCY CHANGE ON BACKSCATTERED POWER.	42
5.3 EFFECT OF INPUT POWER ON TRANSMITTED POWER AND BACKSCATTERED POWER.	43
5.4 VARIATION OF POWER GAIN WITH TIME AND LENGTH	44
5.5 BACKSCATTERED POWER VARIATION WITH TIME FOR DIFFERENT SMF	46
5.6 POWER VARIATION WITH LENGTH FOR FIBRES WITH DIFFERENT PMD.	47
5.7 VARIATION OF BACKSCATTERED POWER AND PUMP FREQUENCY	48
5.8 EFFECT OF FREQUENCY CHANGE ON BACKSCATTERED POWER FOR DIFFERENT TEMPERATURE AND HOW TEMPERATURE AFFECTS THE FREQUENCY SHIFT.....	49
5.9 EFFECT OF TEMPERATURE ON POWER BACKSCATTERED IN THE FIBRE OVER TIME....	50
5.10 EFFECT OF TEMPERATURE ON BACKSCATTERED POWER.....	52

CHAPTER SIX	53
CONCLUSIONS AND RECOMMENDATIONS	53
6.1 CONCLUSION	53
6.2 RECOMMENDATION FOR FURTHER RESEARCH	53
APPENDICES	59

LIST OF FIGURES

Figure 2.1 Schematic of a single fibre optic sensor.....	6
Figure 2.2 Fibre optic sensor using reflection.....	9
Figure 2.3 Interferometric sensor	10
Figure 2.4 Fabry-Perot interferometer-based fibre optic sensors.....	11
Figure 3.1 Brillouin spectrum.....	20
Figure 3.2 Graphical representation of the waves and of the processes involved in stimulated Brillouin Scattering.....	24
Figure 3.3 Generation of Stokes component through Brillouin scattering.....	26
Figure 3.5 Diagram showing the local birefringence in an optical fibre changes the state of polarization of the light from linear to elliptical to circular to elliptical then linear.....	34
Figure 3.6 Effect of PMD in a birefringent fibre on optical pulse.....	37
Figure 4.1 Simulations of parameters affecting Backscattered signal.....	40
Figure 5.2 Change in signal power with change in pump frequency in a fibre.....	42
Figure 5.3 Reflected power and Transmitted power measured as a function of the input power.....	46
Figure 5.4 (a) the signal power change with time.....	47
Figure 5.4 (b) Change of power with PMD coefficients.....	47
Figure 5.4(c) Backscattered power with change in length for different PMD coefficients.....	47
Figure 5.5 Power change against time at different frequencies.....	48
Figure 5.6 (a) Variation of signal power with frequency	49
Figure 5.6 (b): Shows increase in frequency shift with temperature.....	49
Figure 5.7 Variation of power with time at different temperatures.....	50
Figure 5.8 Shows the change in signal power with temperature.....	51

Figure 5.9 Variation of power with temperature..... 52

LIST OF ABBREVIATIONS AND SYMBOLS

BGS- Brillouin Gain Spectrum

BOTDA- Brillouin Optical Time Domain Analysis

BS- Brillouin scattering

CW- Continuous Wave

DFG- Difference-frequency Generation

DGD- Differential Group Delay

DTS- Distributed Temperature sensor

FWHM- Full Width at Half Maximum

GVD- Group Velocity Dispersion

OSA-Optical spectrum Analyzer

OSNR- Optical Signal to Noise Ratio

PC- Polarization Controller

PDL- Polarization Dependent Loss

PMD – Polarization Mode Dispersion

PMF- Polarization Maintaining Fibre

PSP- Principal State of Polarization

SBS- Stimulated Brillouin Scattering

SRS-Stimulated Raman Scattering

SFG- Sum Frequency Generation

SHG- Second Harmonic Generation

SMF- Single Mode Fibre

SNR- Signal to Noise Ratio

SOP- State of Polarization

SRS- Stimulated Raman Scattering

SNR- Signal to Noise Ratio

SMF- Single Mode Fibre

ε_o – Vacuum Permittivity

χ – Magnetic Susceptibility

B – Magnetic field

n – Refractive Index

ω – Angular frequency

A_{eff} -Effective Core Area

L_{eff} -Effective Length

β – Birefringence

γ – Nonlinear Effect

g_B – Brillouin Gain Coefficient

c – Speed of Light

α – Loss Coefficient

Γ – Damping Coefficient

v_A -Acoustic Velocity

γ_e -Electrostrictive Constant

ρ – Density

L_B – Beat Length

Ω_B -Brillouin frequency

\vec{k} -Wave vector

F -Driving force

μ_o – Permeability of free space

ν_B – Brillouin frequency shift

u – potential energy

λ – wavelength

P – Polarization field

I_s – Stokes intensity

I_p – Pump intensity

C_ε – Shift strain coefficient

C_T – Shift temperature coefficient

v_g – Group velocity

ACKNOWLEDGEMENT

I am very grateful to the almighty God for the gift of life and good health throughout my studies. I would also like to express my sincere gratitude to my Supervisors, Dr. Waswa David and Dr. Muguro Ken from whom I received invaluable advice, guidance and all the contributions to this research work. I am also thankful to Physics Department for the opportunity to undertake this project using their available resources. My special thanks also to my husband, my children, my parents, my brothers and sisters for their prayers, continuous encouragement, support and love during the hard times in course of the research. I am also obliged to my colleague's students of University of Eldoret for their unconditional support and encouragement. I thank God for everyone who contributed in any way to the success of this research work.

CHAPTER ONE

INTRODUCTION

1.1 Background

Optical fibres are made from fused silica, and are about the diameter of a human hair and transmit light over long distances with very little loss. They have properties, which are sensitive to environment and are therefore well suited as sensors. Optical sensors have been the subject of interest over the last 20 years [1]. This is due to the fact that they present some distinct advantages over other technologies. The single attractive feature of optical-fibre sensor is their ability to function without any interference with electromagnetic fields. This assists significantly, where long transmission distances of relatively weak signals are essential part of the sensing process [1]. The lack of electrical connections has other broader implications. The optical sensors have major advantages when conductive fluids such as seawater are involved [2]. The optical fibre is remarkably strong, elastic and durable. It has found its place as instrumentation medium for addressing smart structures, where the sensors must tolerate the environment to which the structure is subjected. This allows immunity to large physical strain excursions, substantial temperature excursions, and often a chemical corrosive operating environment [3].

A very important and unique feature of fibre-optic technology consists in its capability for long-range distributed sensing. This feature allows the values of the measurand of interest to be extracted, as a function of position, along the length of the sensing fibre. Distributed sensors are particularly attractive for use in applications where monitoring of measurand is required for a large number of points or continuously over the length of the fibre. Typical examples of application areas include [4]:-Stress monitoring of large structures such as buildings, bridges, dams,

pipelines, ship; Temperature profiling in electrical transformers, generators, process control system and fire detection system; Leakage detection in pipelines; embedded sensors in composite materials for use in real-time evaluation of stress, vibrations and temperature structures and Landslide monitoring.

Distributed sensing techniques are commonly based on light scattering mechanism occurring inside the fibre. One such mechanism is Stimulated Brillouin Scattering, which is as a result of interaction between acoustic waves, a pump wave and Stokes wave. Consequently there is transfer of power between pump and Stokes which simultaneously reinforces the acoustic wave. The Stokes wave is amplified and the pump wave is depleted as they both travel along the fibre. This is true provided that the frequency shift falls within the Brillouin gain spectrum of the fibre itself which is centered at the Brillouin frequency. At each section along the fibre the Brillouin frequency depends on the temperature and strain thus providing the basis for a sensing technique capable of detecting these two parameters [5]. Spontaneous scattering of light is mostly caused by thermal excitation of the medium, and it is proportional to the incident light intensity. On the other hand, the scattering process becomes stimulated if fluctuations in the medium are stimulated by the presence of another electromagnetic wave that reinforces the spontaneous scattering. The scattering process is in the stimulated regime provided that the intensity of the input light has a value above a level known as the threshold, which is lower than the threshold of the spontaneous regime. The stimulated scattering process is readily observed when the light intensity reaches a range between 10^6 and 10^9 Wcm^{-2} [5] and is capable of modifying the optical properties of the material medium.

The stimulated Brillouin scattering (SBS) is a non-linear process that can occur at relatively low power levels. It manifests itself through the conversion of a small

fraction of incident light to scattered light with a shifted frequency. It is affected by the change in refractive index which is registered as a change in Brillouin shift as well as Brillouin backscattered power. The distribution of temperature and strain over long distances can thus be obtained by measuring the change in these parameters. Such sensors are called distributed fibre sensors based on SBS [6].

1.2 Problem Statement.

Optical fibre sensor is designed to monitor physical parameters such as strain and temperature. This can be done along a pipeline, structures and natural calamities (like landslide prone areas). The challenge with the existing sensors like the electrical sensors is that they are not sensitive enough because they have limitation in bandwidth. The existing fibre based sensors are mostly developed using Bragg grating which are not inline sensors hence very expensive.

1.3 Justification

With increasing demand for smart structures, the distributed fibre optic sensor provides the basis for a sensing technique capable of detecting strain and temperature and other physical factors. This sensor solves the challenges experienced when electrical or point sensors are used instead. Its use allows temperature/ strain changes at various points to be monitored at the same point as the power source. This saves time and resources, which would otherwise be used in case of monitoring at different points (point sensors). The proposed study will provide information, which would help in disaster management, which is important in socio-economic development.

1.4 Objectives

- i. To show the existence of stimulated Brillouin scattering in single mode fibres.
- ii. To determine the parameters that affect the backscattered signal power due to stimulated Brillouin scattering.
- iii. To model an optical fibre sensor based on stimulated Brillouin scattering.

CHAPTER TWO

LITERATURE REVIEW

2.1 Introduction

A Sensor is a device that detects and responds to some type of input from the physical environment: - The input could be light, heat, motion and strain. Sensors can either be classified as electrical or optical. This chapter outlines the literature review on limitations of electrical sensor; advantages of optical sensors; different types of fibre optic sensor and the theory Brillouin scattering.

2.2 Electrical Sensors

An electrical sensor detects and respond to a physical parameter (for example: temperature, pressure, humidity, speed) by producing a signal which can be measured electrically. Electrical sensors were the first to be designed and have been used in many applications. However, they suffer from certain limitations some of which include [1]:-

1. The inherent electrical conductivity which makes them susceptible to error causing electromagnetic interference (EMI) thus hard to maintain reliability in electrically hostile conditions;
2. Degradation in harsh environments;
3. Installing a large area with multiple sensors is costly.
4. Finding sensors small and versatile, enough for use in constrained spaces is difficult.
5. Electrical sensors are commonly used for monitoring landslides but they are easily damaged by lightning and electromagnetic noise.

An optical fibre is free from such flaws, and devices using optical fibres have been developed in recent years [1].

2.3 Optical fibres

It is an optical waveguide in the shape of a filament and is generally made of pure glass (although it can be made of plastic materials). An optical fibre is composed of three parts: the core, the cladding, and the coating or buffer [7].

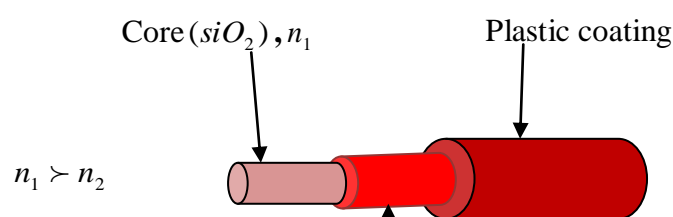


Figure 2.1 Diagram of the structure of an optical fibre.

Where $n_1 > n_2$ means the refractive index of the core is higher than that of cladding.

The core is a cylindrical rod of dielectric material of refractive index, n_1 and is generally made of glass. The cladding layer is made of a dielectric material with a refractive index, n_2 that is less than that of the core material, n_1 . The cladding causes light to be confined to the core of the fibre by total internal reflection at the boundary between the two. The cladding decreases the loss of light from the core into the surrounding air, decreases scattering loss at the surface of the core, protects the fibre from absorbing surface contaminants and adds mechanical strength. The coating or buffer is a layer of plastic used to protect the optical fibre from physical damage. The core and the cladding provide the condition necessary to permit an optical signal to be guided along the optical fibre. The principle of transmission of light along optical fibres is based on total internal reflection. When light is incident from a medium with

high refractive index (n_1) to one with a lower index (n_2), the transmitted beam always emerges at an angle [7].

2.4 Fibre optic sensor

Fibre optic sensor is a system through which a physical, chemical, biological or other quantity interacts with light guided in an optical fibre to produce an optical signal related to the parameter of interest. They are devices that can perform in extreme environmental conditions where other conventional electrical and electronic sensors have difficulties. They can be configured in different shapes to sense various physical disturbances, temperature, strain, pressure, acoustic field among others. In comparison, with other types of sensors, fibre optic sensors exhibit a number of advantages [7]:-

- Small in size and capable of remote sensing.
- Non-conductive and electrically passive which make possible their use in high voltage environment.
- Immune to electromagnetic interference thus is not electrically disturbed by other devices.
- Chemically inert thus can be used in harsh conditions.
- Offer sensitivity to multiple environmental parameters.
- Can be interfaced with data communication system.
- Provide high sensitivity, resolution and dynamic change.

These advantages address the challenges faced by electrical sensors. Fibre optic sensors (FOS) can be used for the measurement of many physical or chemical properties. The principal is based on the fact that light in an optical fibre can be modified in response to an external physical, chemical, biological, biomedical or

similar influence. Most properties can be detected with fibre optic sensors such as strain, pressure, sound, displacement (position), temperature, magnetic field, electric field, chemical analysis, liquid level, rotation, radiation, vibration, among others [7].

2.5 Types of Fibre Optic sensors.

Fibre optic sensors can be specified in terms of types of perturbation or the principle of operation [7]. Thus, they can be described by the chemical concentration, strain, temperature, stress or other physical measurand. The operating principle can be based on variations of intensity, phase, polarization and wavelength. Extrinsic or intrinsic sensors are another classification scheme. In the former, sensing takes place in a region outside the fibre and fibre essentially serves as a conduit for the to-and-fro transmission of light to the sensing region in an efficient and desired form. On the other hand, in an intrinsic sensor one or more of the physical properties of the fibre undergo a change. Fibre optic sensors can also be classified in response to their measurements points. The three important classes here are [7]; point to point sensors, multiplex sensors and distributed sensors. In point to point sensor there is a single measurement point at the end of the fibre optic connection cable, similar to most electrical sensors. Multiplexed sensors allow the measurement at multiple points along a single fibre line and distributed sensors are able to sense at any point over length of fibre.

The common fibre optic sensors (FOS) can be divided into two basic categories [8]: Intensity based sensors and interferometric-based sensors. Generally, intensity modulated FOS are related to the displacement or some other physical perturbation that interacts with the fibre. The perturbation induces light intensity change at the detector. Interferometric-based FOS compares the phase of light in a sensing fibre to a reference fibre in an interferometer [8]. They are much more accurate and sensitive

than intensity-based sensors because the phase of light wave propagating in an optical fibre is more sensitive to external influences than any other parameter and as such, they can be used over a much larger dynamic range. However, since optical phase change cannot be directly detected (optical waves have frequencies in the range of few hundred THz), they require much more complex signal processing techniques which make them expensive.

2.5.1 Intensity-based Fibre Optic Sensor

Intensity-based sensors measure the optical intensity as a function of the perturbing environment [8]. The change of the optical intensity can be related to transmission, reflection, micro bending, or other phenomena such as absorption, scattering, or fluorescence. Intensity-based fibre optic sensors can be divided into reflection sensors, transmission sensors, and micro bending sensors.

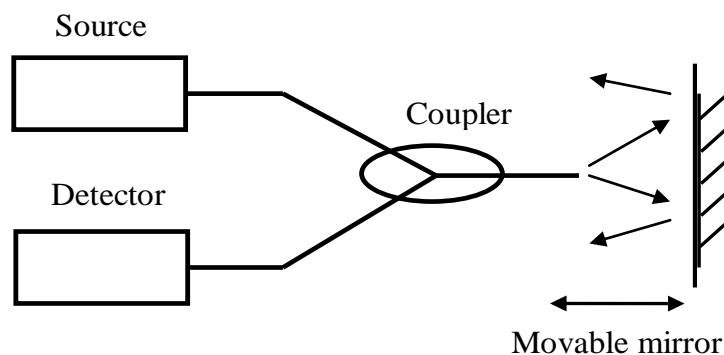


Figure 2.2 Fibre optic sensor using reflection [8].

Light travels along the fibre from left to right, leaves the fibre end, and incidents on a movable reflector. If the reflectors move towards the fibre, most of the light can be reflected back into the fibre so that a high light intensity signal is detected. However, when the reflector moves away from the exit end of the fibre, less light is coupled back into the fibre, and so a weak signal is detected. Therefore, the monotonic relationship between fibre–reflector distance, and reflected light intensity can be used

to measure the displacement distance. To avoid the influence of the intensity fluctuation of the light source, a suitable reference signal is usually added in this type of intensity-based fibre optic sensor. The major problem associated with intensity sensors are random changes of transitivity of optical path and variations of the output power of the optical source, which directly affects the accuracy of the sensor. Intensity sensors therefore need a mechanism that compensates for those changes.

2.5.2 Interferometric-based Fibre Optic Sensor

Interferometric-based sensors take advantage of interferometric techniques to measure pressure, temperature, rotation angle, magnetic field. Generally, the sensor uses a coherent laser source and two single mode fibres. The light is split and put into each fibre. If the environment perturbs one fibre relative to the other, a phase shift occurs that can be detected precisely. The shift of the phase is detected by an interferometer. There are four interferometric configurations: the Mach-Zehnder, the Michelson, the Fabry-Perot, and the Sagnac [8].

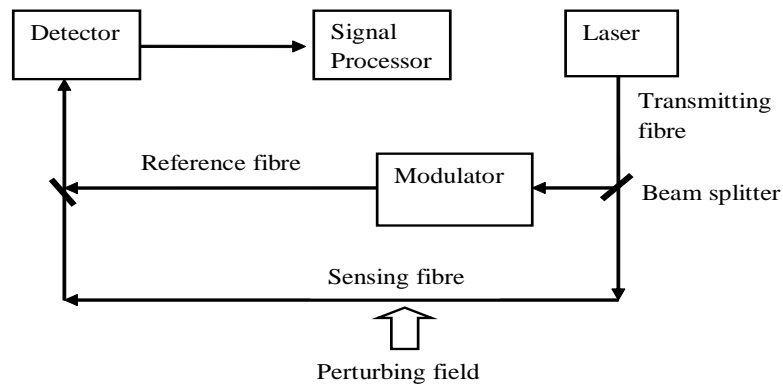


Figure 2.3 Interferometric sensor [8].

The laser beam from the light source splits at the beam splitter so that light travels in the reference single mode fibre and the sensing fibre, which is exposed to the perturbing environment. If the light in the sensing fibre and the light in the reference fibre are exactly in phase after recombining, they constructively interfere and the

output signal intensity is high. If they are out of phase, destructive interference happens and the received optical intensity is lower. Such devices have a phase shift if the sensing fibre has a length or refractive index change, or both.

In the Fabry-Perot interferometer, a multiple-beam is used. Figure 2.4 shows a fibre optic Fabry-Perot interferometer. Due to the high reflectivity of the mirrors, light bounces back and forth in the cavity many times, increasing the phase delay many times. The transmitted output intensity of the Fabry-Perot interferometer is given by the fact that the higher the reflection coefficient (F_c), the sharper the interference peak will be. In other words, near the peak region, the output light intensity is very sensitive to the small change in the phase delay.

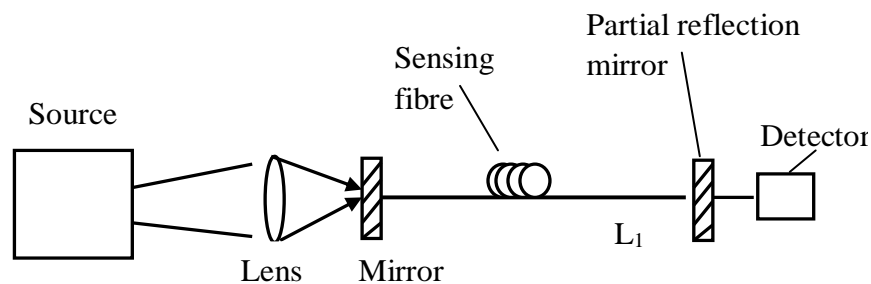


Figure 2.4 Fabry-Perot interferometer-based fibre optic sensors [9].

The larger the F_c number, the sharper the interference peak will be. Thus, the sensitivity of a Fabry-Perot interferometer-based fibre sensor can be much higher than that of the Mach-Zehnder or Michelson interferometer.

In summary, fibre optic interferometric sensors usually have the advantage such as the design flexibility, the large dynamic range and high resolution. However, because of the nonlinear periodic characteristic of the interference signal, the accurate detection of the differential phase change of an interferometer turns to be a real challenge [8].

2.5.3 Polarization-based Fibre Optic Sensor(PFOS)

In spite of many advantages, there is a growing demand for improved sensitivity, reliability, accuracy, flexibility and better compatibility of fibre optic sensors for various applications. Among the various optical sensor designs, polarimetric fibre optic sensor (PFOS) has its unique advantages over the rest. When a force is applied along the length of a polarimetric fibre, an additional birefringence is introduced due to the elasto-optic effect. In many cases, the stress or strain in different directions is different, so that the induced refractive index change is also different in different directions. Thus, there is an induced phase difference between different polarization directions. In other words, under the external perturbation, such as stress or strain, the optical fibre works like a linear retarder. Therefore, by detecting the change in the output polarization state, the external perturbation can be sensed [8]. To make the fibre optic sensor practical, it is necessary to display sensitivity to the phenomenon designed to measure insensitivity to changes in other environmental parameters. For the strain or stress measurement, environmental temperature is unwanted external parameter. For PFOS, environmentally induced refractive index changes in the two polarization directions are almost the same. Thus, there is almost no induced phase difference between two polarization states and thus environmental temperature fluctuation will not substantially deteriorate the sensor's performance.

2.6 Theory of Brillouin Scattering

Brillouin scattering is a nonlinear process that can occur in optical fibres at large intensity. The large intensity produces compression in fibre core through a process known as electrostriction [9]. This phenomenon produces intensity fluctuations in fibre medium. It increases the material disorder, which in turn modulates linear refractive index of medium and results in electrostrictive nonlinearity. The modulated

refractive index behaves as an index grating, which is power induced. The scattering of pump light through Bragg diffraction by the pump induced index grating is called Brillouin scattering. The disorder is time dependent so the scattered light is shifted in frequency (Brillouin shift) by the frequency of sound wave. Quantum mechanically, the Brillouin shift originates from photon to phonon interaction and is associated by Doppler displacement. In this interaction either a phonon is annihilated (stokes process-positive Brillouin shift) or created (antistokes process-negative Brillouin shift) [2].

The concept of using Brillouin scattering in fibre for optical sensing was first proposed in 1989 [1, 5, 21] and it was termed Brillouin optical time domain analysis (BOTDA), using the pump-probe wave approach. This basic approach involved launching a short pump pulse into one end of the test fibre and a continuous wave (CW) probe beam into the other end. If the probe wave is at the Stokes frequency, then energy flows from the pump to the Stokes wave providing Brillouin gain to this CW wave. If the probe wave instead takes the anti-Stokes frequency, it then gives energy to the pump wave (pulsed signal), and the detected CW signal experiences a Brillouin loss. The frequency difference between the two lasers could be set to a particular value corresponding to the Brillouin frequency of the optical fibres, and the CW probe would experience gain varying along the fibre. The gain as a function of position along the fibre could thus be determined by the time dependence of the detected CW light. By measuring the time dependent CW signal over a wide range of frequency differences between the pump and probe, the Brillouin frequency at each fibre location could be determined. This allowed mapping the strain or temperature distribution along the entire fibre length.

The first strain distribution measurement was reported on submarine cables [2] using distributed fibre sensors based on Brillouin scattering. The reported strain distribution was obtained over a 1.3-km cable [3]. Later, another strain measurement on the bent slot-type optical cables was reported [4]. Temperature measurement using Brillouin scattering was proposed in 1989 [5, 1, 21] utilizing the linear relationship between Brillouin frequency shift and temperature in a single mode fibre and measured with a Fabry-Perot interferometer. A distributed temperature measurement on a 1.2 km single mode fibre with a 3 °C temperature resolution and a 100 m spatial resolution was demonstrated with a BOTDA system [6]. This performance was further improved to achieve a 22 km sensing length with 5 m spatial resolution of 1 °C temperature resolution [7]. The next development in BOTDA was the use of Brillouin loss rather than Brillouin gain [8] in order to increase the sensing length. Relative to the pulsed pump wave, the CW probe wave has been set at the anti-Stokes frequency instead of the Stokes frequency; hence the detected signal is a Brillouin loss. The difference between the gain and loss is the pulse signal that has been switched from donor to receiver with respect to energy exchange. For long sensing lengths (>10 km), there are two limitations of the former method: (1) peak pulse power of the pump must be lower than the stimulated Brillouin scattering (SBS) threshold; and (2) the finite energy of pump pulses can become significantly depleted, leading to uneven gain along the sensing fibre excessive depletion occurs at the beginning. Under the Brillouin loss regime, the CW probe therefore experienced loss at locations along the fibre at which the frequency difference between the lasers matched the local Brillouin frequency of the fibre. As it is much harder to deplete the CW rather than a pulsed pump, a longer sensing length of 50 km with 5 m spatial resolution and 1 °C temperature resolution was reported using the Brillouin loss mechanism [8]. The

longest reported distributed sensor length using BOTDR is 57 km with a spatial resolution of 20 m and 3 °C temperature resolution [9]. More recently, a sensing length of 150 km was demonstrated by amplifying the BOTDR signal using Raman amplifiers in the fibre [10]; a temperature resolution of 5.2 °C was achieved with a 50 m spatial resolution. The better spatial resolution in BOTDA is attributed by the pump and probe wave interaction induced Brillouin amplification over the entire sensing length, while in BOTDR only one pump pulse is used and it works in spontaneous Brillouin scattering regime.

In this work, the frequency difference between pump and probe signal was set from the two laser sources. This frequency difference can be swept in the spectral range of the Brillouin frequency shift (10.5 to 11 GHz) so that the frequency response of the fibre can be determined. In other words the magnitude of the interaction between pump and probe is recorded at every location along the optical fibre. The local Brillouin frequency shift which contains the temperature/strain information is found to be at the maximum of the resonant interaction between both optical signals.

CHAPTER THREE

THEORY

3.1 Introduction

Stimulated Brillouin scattering (SBS) is a process in which two counter-propagating light waves, at different frequencies, interact with an acoustic wave. This chapter explains the phenomenon of SBS and factors that influence it in optical fibres.

The nonlinear scattering effects in optical fibres are due to the inelastic scattering of a photon to lower energy photon. The energy difference is absorbed by the molecular vibrations or phonon in the medium. In other words, the energy of the light waves is transferred to another wave, which is at a higher wavelength such that the energy difference appears in the form of phonons [3]. The other wave is known as the Stokes wave. High-energy photon at anti-stokes frequency can also be created if phonon of right energy and momentum is available. There are two inelastic nonlinear scattering phenomena in optical fibres and both are related to vibration excitation modes of silica [2,4]. These phenomena are known as Stimulated Raman Scattering (SRS) and Stimulated Brillouin Scattering (SBS). The fundamental difference is that, optical phonons are involved in SRS while SBS occur through acoustic phonons. As a result of this difference, SBS occurs only in backward direction while SRS can occur in both forward and backward directions. The nonlinear scattering process causes a disproportionate attenuation at high optical power levels. It also causes the transfer of power from one signal to other modes in forward and backward direction. The two stimulated scattering mechanism (SBS and SRS) also provides optical gain but with shift in frequency.

The fundamental equation describing wave propagation in a medium is given by [9]:

$$\nabla^2 \vec{E} - \frac{1}{C_o^2} \frac{\partial^2 \vec{E}}{\partial t^2} = \mu_o \frac{\partial^2 \vec{P}}{\partial t^2} \dots\dots\dots(3.1)$$

Where μ_o - Permeability of free space, E - Electric field intensity, C_o - Speed of light in a vacuum, P - Polarization field and t - Change in time.

The relation between polarization and incident field at high light intensity is written as:

$$\vec{P} = \epsilon_o [\chi^{(1)} \vec{E} + \chi^{(2)} \vec{E}^2 + \chi^{(3)} \vec{E}^3 + \dots] \dots\dots\dots(3.2)$$

Where χ - Nonlinear susceptibilities, P - Polarization field and E - Electric field intensity.

With this form of polarization, (3.1) can be written as:

$$\nabla^2 \vec{E} + \frac{\epsilon^{(1)}}{C_o^2} \frac{\partial^2 \vec{E}}{\partial t^2} = \mu_o \frac{\partial^2 \vec{P}^{NL}}{\partial t^2} \dots\dots\dots(3.3)$$

The nonlinear polarization (terms of order 2 and more in E) causes coupling between individual spectral components. Its impact is illustrated by introduction of nonlinear susceptibilities $\chi^{(n)}$ into equation (3.1) and considering that the incident light wave consists only of two monochromatic waves. Then,

$$\vec{E}(r,t) = \vec{E}(r) \exp(-i\omega_1 t) + \vec{E}(r) \exp(-i\omega_2 t) + c.c. \dots\dots\dots(3.4)$$

Where c.c stands for complex conjugate.

Then second order nonlinear polarization is given by :-

$$\begin{aligned} \chi^{(2)} \vec{E}^2 = & \{ \chi^{(2)} \vec{E}_1^2 [\exp(-2i\omega_1 t) + \vec{E}_2^2 \exp(-2i\omega_2 t)] + \{ 2 \vec{E}_1 \vec{E}_2 \exp\{-i(\omega_1 + \omega_2)t\} \\ & + 2 \vec{E}_1 \vec{E}_2^* \exp\{-i(\omega_1 - \omega_2)t\} + \dots \} + \{ 2 \chi^{(2)} [\vec{E}_1 \vec{E}_1^* + \vec{E}_2 \vec{E}_2^*] \} \dots \dots \dots (3.5) \end{aligned}$$

The first term containing two oscillating terms at frequencies $2\omega_1$ and $2\omega_2$ is responsible for second-harmonic generation (SHG). In second term, components oscillate at the sum and at the difference of the original frequencies. They correspond to sum-frequency generation (SFG) and difference frequency generations (DFG) [9]. The last two terms are constant and cause optical rectification, that amounts to the presence of a static electric field in the medium. The above processes are parametric (state of medium where it takes place remain the same). Brillouin Scattering is a nonparametric process, that is; there is net modification of the energy state of the medium.

For an oscillating electric field at pump frequency ω_p , the electrostriction process produces macroscopic acoustic wave at some frequency ω_B . The Brillouin scattering may be spontaneous or stimulated. In spontaneous scattering there is annihilation of pump photon, which results in creation of stokes photon and acoustic phonon simultaneously. The conservation laws of energy and momentum must be followed in such scattering process. For energy conservation, the stokes shift ω_B must be equal to $(\omega_p - \omega_s)$ where ω_p and ω_s are frequencies of pump and stokes waves respectively.

The momentum conservation requires; $\vec{k}_A = \vec{k}_p - \vec{k}_s$

Where $\vec{k}_A, \vec{k}_p, \vec{k}_s$, are wave vectors of acoustic pump and stokes waves respectively. If

v_A is acoustic velocity then the dispersion relation can be written as

$$\omega_B = v_A |\vec{k}_A| = v_A |\vec{k}_P - \vec{k}_S| \quad \text{or} \quad \omega_B = 2v_A |\vec{k}_P| \sin \theta / 2 \dots \dots \dots (3.6)$$

Where ω_B is the stokes shift and θ is the angle between the pump and stokes momentum vectors and modulus of k_p and k_s is taken as nearly equal. From the above expression, it shows that frequency shifts depends on angle θ , for $\theta = 0^\circ$, shift is zero. That there is no frequency shift in forward direction (no Brillouin Scattering).

When $\theta = \pi$ means backward direction and in this situation the shift is maximum in the backward direction. The frequency shift $\nu_B = \frac{\omega_B}{2\pi}$ is calculated from equation

$$(3.6) \text{ and from the relationship } |\vec{k}_p| = \frac{2\pi n}{\lambda_p} \text{ then} \quad \nu_B = \frac{2n v_A}{\lambda_p} \dots \dots \dots (3.7)$$

Where n the mode index and λ_p is the wavelength of the pump and v_A is acoustic wave velocity.

In single mode fibres, the spontaneous Brillouin scattering (BS) may also occur in forward direction due to guided nature of acoustic waves. In this case a small amount of extremely weak light is generated and scattered light wave is produced spontaneously. This interferes with pump signal. The interference generates spatial modulation in intensity, which results in amplification of acoustic wave by electrostriction effect (elasto-optic effect). The amplified acoustic wave in turn raises spatial modulation intensity and hence the amplitude of scattered wave. This causes an increment in amplitude of acoustic wave. This positive feedback dynamics is responsible for SBS. That is, optical pump wave is scattered by acoustic waves

leading to stokes (a longer wavelength than that of the pump) or anti-stokes (a shorter wavelength than that of the pump) components as shown in Figure 3.1 below:-

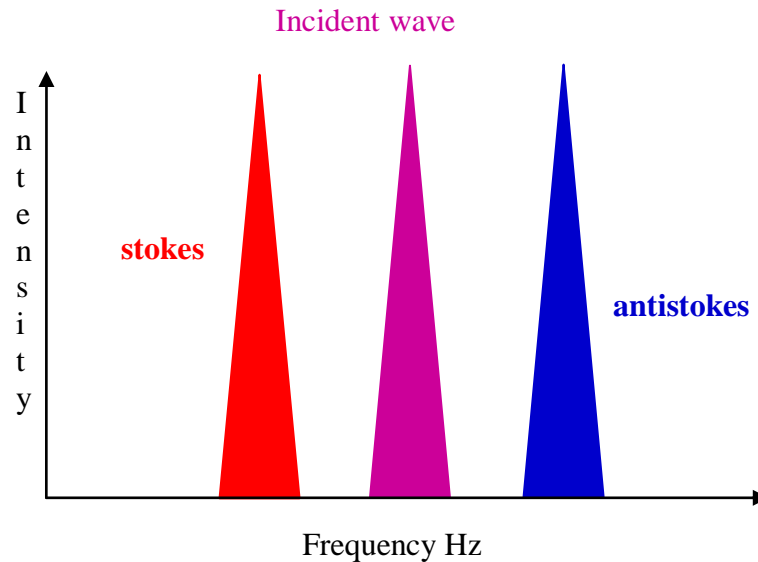


Figure 3.1 Brillouin spectrum

Essentially, Scattering occurs as a result of a Bragg-type reflection from moving diffraction gratings created from the refractive- index variations, causing acoustic waves propagating axially in the fibre. These acoustic waves can be generated spontaneously by thermal excitation and when this is the case, the resulting scattering effect on optical waves is known as ‘spontaneous’ Brillouin scattering. Thus the stokes scattered wave will be as a result of axially propagating acoustic wave moving away from an optical pump pulse and anti-stokes wave from one moving towards it.

3.2 Coupled-Wave Equations

SBS is a nonlinear process that obeys equation 3.3 ,yet the nonlinear polarization that is responsible for coupling of the two optical frequencies is not due to non susceptibility as in parametric but due to presence of sound waves. The description of

SBS is shown by the equations of propagation for the pump, stokes and acoustic waves below [10]:-

$$\nabla^2 \vec{E}_1 + \frac{\epsilon^{(1)}}{c_o^2} \frac{\partial^2 \vec{E}}{\partial t^2} = \mu_o \frac{\partial^2 \vec{P}_1^{NL}}{\partial t^2} \dots\dots\dots 3.8$$

$$\nabla^2 \vec{E}_2 + \frac{\epsilon^1}{c_o^2} \frac{\partial^2 \vec{E}_2}{\partial t^2} = \mu_o \frac{\partial^2 \vec{P}_2^{NL}}{\partial t^2} \dots\dots\dots 3.9$$

$$\nu^2 \nabla^2 \Delta \rho + \Gamma \nabla^2 \frac{\partial}{\partial t} \Delta \rho = \Delta F \dots\dots\dots 3.10$$

where, $\Delta \rho$ is density variation, Γ is acoustic damping coefficient, F is driving force, E -electric field, P -Polarization field, μ_o - Permeability of free space, C_o - Speed of light in a vacuum. In equation (3.10) the density variation has been used to describe acoustic wave. Only the case of backscattering is considered and the polarizations of the two light waves are parallel to the unitary vector e_1 . For stokes scattering where $\omega_1 = \omega_2 + \Omega$, the sound waves propagate in the same direction as E namely $+z$ direction. and can be written as;

$$\vec{E}_1(r, t) = e_1 E_1(z, t) \exp[i(k_1 z - \omega t)] + c.c. \dots\dots\dots (3.11a)$$

$$\vec{E}_2(r, t) = e_1 E_2(z, t) \exp[i(-k_2 z - \omega_2 t)] + \Delta e(r, t) = A(z, t) \exp[i(qz - \Omega t)] + c.c. \dots\dots (3.11b)$$

The rapidly oscillating parts of 3.11 describe the plane waves that would be solutions of (3.8) to (3.10) in the absence of source terms. E_1, E_2 and A are slowly-varying envelopes of the waves, caused by coupling [10].

3.3 Electrostriction

It is basically the tendency of molecules to move or reorient in the presence of an electric field in order to minimize potential energy. When the density of a material increases by $\Delta\rho$, its dielectric constant changes by an amount given by:-

$$\Delta\varepsilon = \frac{\partial\varepsilon}{\partial\rho} \Delta\rho \dots\dots\dots(3.12)$$

ε is the dielectric constant.

The potential energy per unit volume u depends on the dielectric constant as shown below:

$$u = \frac{\varepsilon E^2}{8\pi} \dots\dots\dots(3.13)$$

The increase in energy induced by the densification is

$$\Delta u = \frac{E^2}{2} \Delta\varepsilon = \frac{E^2}{2} \frac{\partial\varepsilon}{\partial\rho} \Delta\rho \dots\dots\dots(3.14)$$

From the first law of thermodynamics, this change must be equal to the work done in compressing the material per unit volume is given by:

$$\Delta w = P_{st} \frac{\Delta V}{V} = -P_{st} \frac{\Delta\rho}{\rho} \dots\dots\dots(3.15)$$

Where P_{st} is the contribution of the electric field to the pressure of the material and the minus sign of P_{st} , shows that the total pressure is reduced in regions of high electric field and the molecules of the material are drawn towards these regions.

From Equation 3.14 and 3.15 we obtain:

$$P_{st} = -\rho \frac{\partial\varepsilon}{\partial\rho} \frac{E^2}{2} = -\gamma_e \frac{E^2}{2} \dots\dots\dots(3.16)$$

where the electrostrictive constant $\gamma_e = \rho \frac{\partial\varepsilon}{\partial\rho}$.

From the coupled equations,

$$\frac{\partial E_1}{\partial z} + \frac{n}{C_o} \frac{\partial E_1}{\partial t} = \frac{i\omega\gamma_e}{2nC_o\rho} A E_2 \dots\dots\dots(3.17)$$

$$\frac{\partial E_2}{\partial z} - \frac{n}{C_o} \frac{\partial E_2}{\partial t} = \frac{i\omega\gamma_e}{2nC_o\rho} A^* E_1 \dots\dots\dots(3.18)$$

$$\frac{\partial A}{\partial z} + \frac{1}{v} \frac{\partial A}{\partial t} + \frac{\Gamma q^2}{v} A = \frac{iq\gamma_e}{v^2} E_1 E_2^* \dots\dots\dots(3.19)$$

Where optical frequencies are very close thus $\omega_1 \approx \omega_2 = \omega$.

The interference pattern of \vec{E}_1 and \vec{E}_2 , is transformed by the electrostriction into a density variation of the medium i.e. sound wave. The diffraction of \vec{E}_1 on this sound wave reinforces \vec{E}_2 , that in turn increases interference as shown in figure 3.2 [10]:-

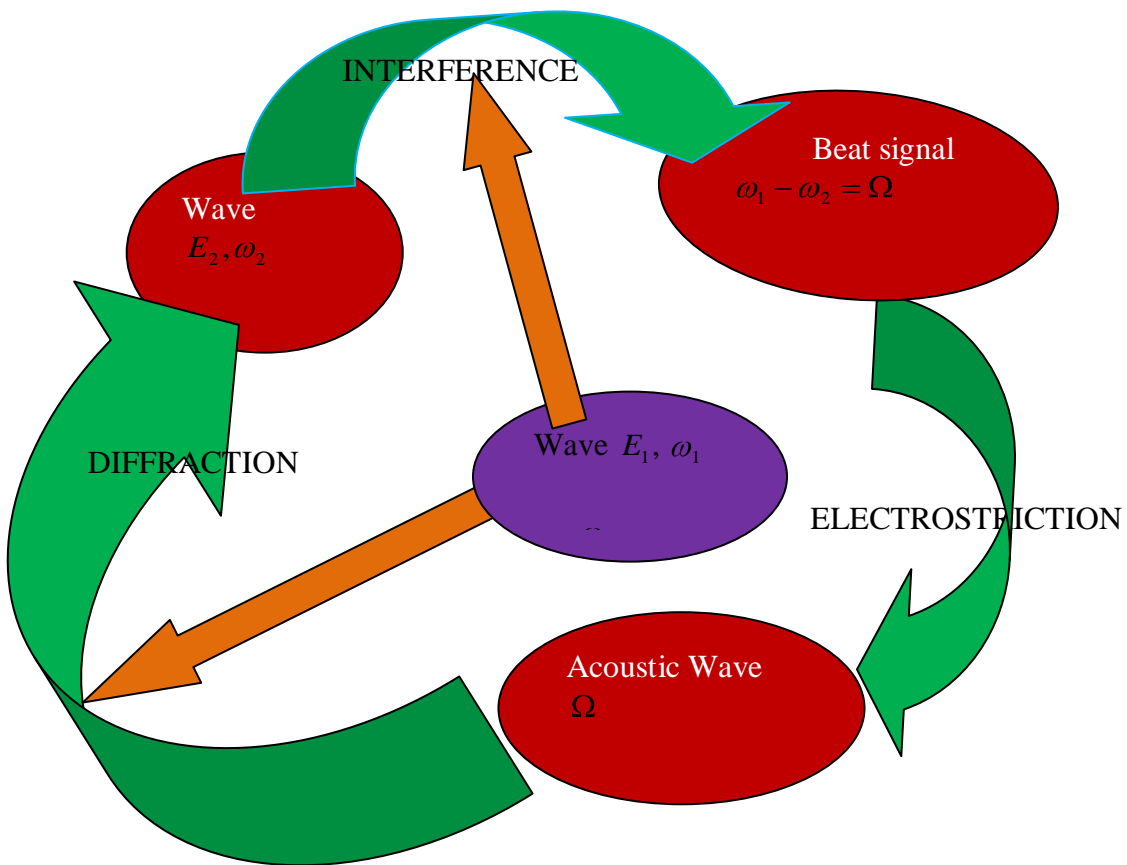


Figure 3.2 Graphical representation of the waves and of the processes involved in stimulated Brillouin Scattering [10].

3.4 Stimulated Brillouin Scattering

The process of SBS is described as a nonlinear interaction between the pump and stokes field through an acoustic wave by the process of electrostriction. The acoustic wave in turn modulates the refractive index of the medium [11]. The scattering process is annihilation of the pump photon and acoustic phonon simultaneously. As both the energy and the momentum must be conserved during each scattering event, the frequencies and

the wave vectors of the three waves are related by:

$$\Omega_B = \omega_p - \omega_s \dots\dots\dots(3.20a)$$

$$k_A = k_p - k_s \dots\dots\dots(3.20b)$$

where ω_p and ω_s are frequencies and k_p and k_s are the wave vectors, of the pump and stokes waves respectively.

The frequency Ω_B and the wave vector k_A of the acoustic wave satisfy the standard dispersion relation

$$\Omega_B = v_A |k_A| \approx 2v_A |k_p| \sin \left(\frac{\theta}{2} \right) \dots\dots\dots(3.21)$$

where θ angle between the pump and stokes field and v_A is the acoustic velocity.

From equation (3.21), $|k_A| \approx |k_s|$, The frequency shift experienced by the stokes wave as a function of scattering angle θ is illustrated in figure 3.3 below: -

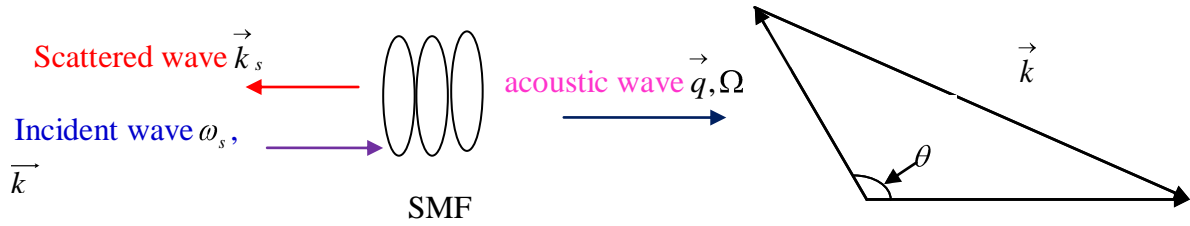


Figure 3.3 Illustration of the generation of stokes component through Brillouin scattering. [12].

From equation 3.21, the frequency shift of the stokes wave depends on the scattering angle. Ω_B is maximum in the backward direction ($\theta = \pi$) and vanishes in the forward direction ($\theta = 0$). Thus SBS occurs only in the backward direction with the Brillouin shift given by:-

$$\nu_B = \frac{\Omega_B}{2\pi} = \frac{2n_p v_A}{\lambda_p} \dots\dots\dots 3.22$$

where n_p is the effective mode index at pump wavelength λ_p . For silica fibre $\nu_B = 11\text{GHz}$ at $\lambda_p = 1.55\text{nm}$ [13].

Brillouin scattering in optical fibres is stimulated through the use of pulsed probe wave and counter propagating CW pump wave. The interaction between the two waves is accurately described by the steady-state SBS equation [6],

$$\frac{dI_S}{dz} = -g_B I_P I_S + \alpha_S I_S \dots\dots\dots (3.23)$$

$$\frac{dI_P}{dz} = -g_B I_S I_P - \alpha_P I_P \dots\dots\dots (3.24)$$

where α is the fibre loss coefficient and g_B is the Brillouin gain coefficient.

The dependence of Brillouin gain on pump probe frequency shift is usually described by Lorentzian profile [9]. The Brillouin gain spectrum (BGS) profile, $g(\nu)$ is given by:-

$$g(\nu) = \frac{\gamma g_o}{1 + \frac{4[\nu - \nu_B(T, \varepsilon)]^2}{\Delta \nu_B^2}} \dots \dots \dots (3.25)$$

where $\Delta \nu_B$ is the Full Width Half Maximum (FWHM) Brillouin gain line width, g_o is the peak gain, γ is polarization factor, which accounts for the dependence of gain on the polarization of the two beams, ν is the frequency difference between the lasers and $\nu_B(T, \varepsilon)$ is the temperature/strain dependent Brillouin frequency shift. The relation between ν_B and temperature/strain can be written as:

$$\nu_B(\Delta T, \Delta \varepsilon) = \nu_{BO} + C_T \Delta T + C_\varepsilon \Delta \varepsilon \dots \dots \dots (3.26)$$

Where ν_{BO} represents the Brillouin frequency of the unperturbed fibre, which is for a fixed temperature and strain. ΔT and $\Delta \varepsilon$ are changes in temperature and strain while C_T and C_ε are the temperature shift and /strain shift coefficients respectively. The typical values for these coefficients at a wavelength $\lambda = 1.32 \mu\text{m}$ are $C_\varepsilon = 594.1 \text{MHz}$ and $C_T = 1.36 \text{MHz}$ [14].

At low guided light intensity, spatial fluctuations of the refractive index in the optical fibre scatter light that travels along the fibre core in all directions. This occurrence is referred to as Rayleigh scattering [15]. Rayleigh scattering is also a linear scattering process but the nonlinear Brillouin scattering has a power threshold much above the occurrence of the linear Rayleigh scattering.

3.5 Stimulated Brillouin Threshold Power

Taking into consideration the Brillouin interaction between the pump and stokes wave, the initial growth of stokes wave under continuous wave (CW) and quasi continuous wave (QCW) condition, can be written as:

$$\frac{dI_s}{dz} = g_B I_p I_s \dots\dots\dots(3.27)$$

Where g_B the Brillouin is gain coefficient, I_p and I_s are the pump and stokes waves intensity respectively. The Brillouin scattering process produces photons within the bandwidth of Brillouin gain spectrum and hence all frequency components will be amplified. The frequency component for which g_B is maximum builds up rapidly and increases exponentially. For pure silica, g_B is maximum for frequency component which is downshifted from pump frequency by about 11GHz. Considering the fibre losses at stokes frequency and counterpropagating nature of stokes wave, Equation (3.27) can be written as:

$$\frac{dI_s}{dz} = -g_B I_p I_s + \alpha_s I_s \dots\dots\dots$$

(3.28)

For pump wave the coupled equation can be written as:

$$\frac{dI_p}{dz} = -\frac{\omega_p}{\omega_s} g_B I_p I_s - \alpha_p I_p \dots\dots\dots$$

(3.29)

where α_p is the fibre losses at pump frequency for a fibre length of z. From equations (3.28) and (3.29), two conditions have been used for simplifications: the first is $\omega_p \approx \omega_s$ owing to a relatively small value of the Brillouin shift and the second is $\alpha_p = \alpha_s = \alpha$, for same reason that, fibre losses are nearly the same for the pump and

stokes waves. Therefore in the absence of fibre losses ($\alpha = 0$), Equation (3.28) and (3.29) are reduced to;-

$$(I_p - I_s) = \text{constant} \dots \dots \dots (3.30)$$

This expression describes the conservation phenomenon on light energy during the Brillouin process. Threshold power is the minimum power level at which the effect of nonlinearity starts. It is the incident power at which the pump and the stokes powers are equal to the fibre output. In case the stokes power is much smaller than the pump power, pump depletion can be neglected. Using $I_p(z) = I_p(0)e^{-\alpha z}$ in equation (3.29) and integrating it over the fibre length L, the stokes intensity is found to grow exponentially in the backward direction as:-

$$I_s(0) = I_s(L) \exp(g_B P_o L_{eff} / A_{eff} - \alpha L) \dots \dots \dots (3.31)$$

Where $P_o = I_p(0)$ is the input pump power, A_{eff} is the effective mode area and L_{eff} is the effective length of interaction for a fibre length L is defined by [16].

$$I_p = I_p(0) \exp[-\alpha z] \dots \dots \dots (3.32)$$

Equation (3.32) shows how a stokes signal incident at $z=L$, grows in backward direction because of Brillouin amplification occurring as a result of SBS. Equation (3.31) and (3.32) can be written as:-

$$P_s(o) = P_s(L) \exp(-\alpha L) \exp \frac{(g_B P_p(0) L_{eff})}{A_{eff}} \dots \dots \dots (3.33)$$

and

$$P_p(L) = P_p(0) \exp[-\alpha L] \dots \dots \dots (3.34)$$

where the pump and stokes intensities are related to power as $P_s = A_{eff} I_s$ and $P_p = A_{eff} I_p$ respectively.

The threshold power can be calculated from equation (3.33) and (3.34) and can be approximated as:-

$$P_{th} = \frac{21bA_{eff}}{g_B L_{eff}} \dots\dots\dots(3.35)$$

Where b is known as polarization factor and its value lies between 1 and 2 depending on relative polarization of pump and stokes waves[16]. Typically $A_{eff} \approx 50 \mu m, L_{eff} = 20 km$ and $g_B = 4 \times 10^{-11} m/W$ for optical system at 1550nm, for $b=1$ $P_{th} \approx 1.3 mW$. Because of such a low value of P_{th} , SBS process is a dominant nonlinear process in fibres. It depends mainly on g_B and the fibres homogeneity affects g_B and hence P_{th} . Variation in dopants also affects SBS threshold power up to some extent [16].

3.6 Brillouin Gain Spectrum

In SBS, the growth of stokes is characterized by the Brillouin –gain spectrum $g_B(\omega)$ peaking at $\omega = \omega_B$ and the spectral width of the gain spectrum is very small. It is related to the damping time of acoustic wave and the phonon lifetime [8]. When the acoustic waves decay as $\exp(-\Gamma_B t)$, the Brillouin gain has a Lorentzian spectrum of the form:-

$$g_B(\Omega) = \frac{g_B(\Gamma_B/2)^2}{(\omega - \omega_B)^2 + (\Gamma_B/2)^2} \dots\dots\dots(3.36)$$

where the peak value of the Brillouin gain at $\Omega = \Omega_B$ is given by:-

$$g_p \equiv g_B(\Omega_B) = \frac{8\pi^2 \gamma_e^2}{n_p \lambda_p^2 \rho_o C v_A \Gamma_B} \dots\dots\dots(3.37)$$

where $\gamma_e \approx 0.902$ is electrostrictive constant of silica and $\rho_o \approx 2210\text{kg/m}^3$ is its density [17]. The FWHM of the gain spectrum is related to Γ_B as $\Delta\nu_B = \Gamma_B/2\pi$. The phonon lifetime, $T_B = \Gamma_B^{-1}$ is typically $< 10\text{ns}$ [18]. The $g_B(\Omega_B)$ depends on many parameters like concentration of dopants, inhomogeneous distribution of dopants and the electrostrictive coefficient. For pure silica, g_B is maximum for frequency component which is downshifted from pump frequency by about by 11GHz [19,20].

3.7 Distributed Optical Fibre Sensor Based on Stimulated Brillouin Scattering

A device or a system capable of detecting, measuring and reproducing a particular physical or chemical variable (measurand) in the electrical domain may be recognized as a sensor or sensor system. If light is used in such a sensor and the measurand changes some of the light properties, the device is known as optical sensor. These changes on light properties usually happen in the transducer part of the sensor. These sensors are capable of detecting and measuring variables along a fibre that acts both as a distributed transducer and as an optical channel.

3.8 Sensing Principle

The operation of distributed fibre sensor based on SBS relies on the dependence of the Brillouin frequency shift, ν_B on the velocity of ν_A of acoustic waves in the fibre, that is[3];

$$\nu_B(z) = \frac{2n_{eff}(z)v_a}{\lambda} \dots\dots\dots(3.38)$$

Where

ν_a - Velocity of sound in glass

λ -free space wave length

n_{eff} is effective refractive index of the fibre as a function of position z .

The Brillouin frequency shift depends on both the effective refractive index of the fibre mode and the velocity of acoustic waves within the fibre. It changes whenever these quantities change in response to local environmental variations and can be used to deduce the temperature or strain along the fibre. From experiments, there is linear relationship between the Brillouin frequency shift and temperature or strain [3].

3.9 Brillouin Optical Time Domain Analysis (BOTDA)

The concept of using SBS in optical fibres for optical sensing was first proposed in 1989 [1, 5, 21] and it was termed as BOTDA. Using the pump-probe wave approach BOTDA based systems work on the principle of Brillouin amplification. They consist of two lasers injecting light from opposite ends of the fibre at frequencies ω_1 (probe laser) and ω_2 (pump laser). The frequencies of the lasers are adjusted such that $\omega_2 = \omega_1 + \nu_B$. This results in the probe light having the same frequency as that of the Brillouin scattered light generated by the pump laser. The probe intensity is thus added to the pump scattering intensity resulting in stimulated scattering of the pump. The frequency difference between the lasers could be set to a particular value corresponding to the Brillouin frequency of the optical fibre, and the CW probe would experience gain varying along the fibre. The gain as a function of position along the fibre could thus be determined by the time dependant CW signal over a wide range of frequency differences between the pump and the probe; the Brillouin frequency at each fibre location could be determined. This allowed to mapping of temperature distribution along the entire fibre length [22].

3.10 Birefringence

It is defined as the difference in refractive indices of a pair of orthogonal polarization states. The propagation constant β , for the orthogonal polarization mode is given by[23]:-

$$\Delta\beta = \beta_s - \beta_f = \frac{\omega n_s}{c} - \frac{\omega n_f}{c} = \frac{\omega \Delta n}{c} = \frac{2\pi}{\lambda} \Delta n$$

.....(3.39)

where $\Delta n = n_s - n_f > 0$ is the birefringence, λ - wavelength of light in vacuum.

Any optical wave of arbitrary polarization can be represented as the linear superposition of two orthogonally polarized HE_{11} modes in a waveguide. In ideal case, where the waveguide has cylindrical symmetry, these two modes are indistinguishable or degenerate in terms of the propagation properties. The loss is due to fibre birefringence. Birefringence can be affected by both intrinsic and extrinsic factors. Intrinsic factors like non-circular core or built in asymmetric stress in a fibre resulting from processes during the fibre's manufacture. A non-circular core gives rise to geometric Birefringence whereas non-symmetrical stress field creates birefringence. These factors cause the index of one polarized mode to differ slightly from other, resulting in different propagation velocities for the two modes. A light pulse travelling along the polarization mode with smaller refractive index travels with fast speed and that polarization mode is termed as fast axis and the other as slow-axis as shown in figure 3.5 [24].

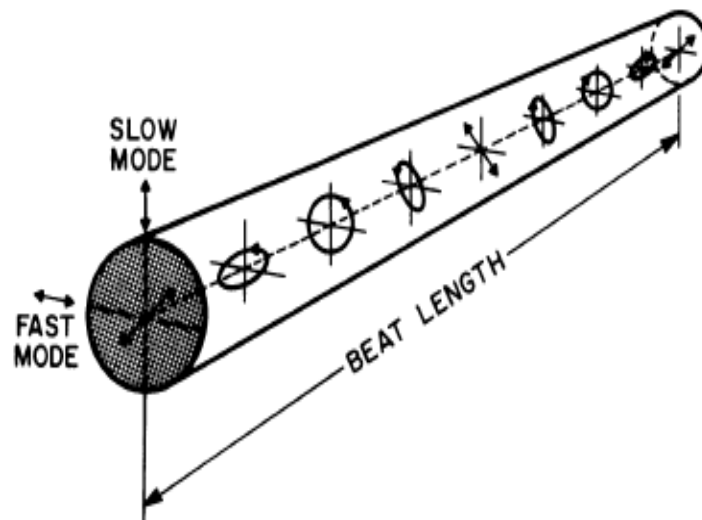


Figure 3.5 Illustration of how local birefringence in an optical fibre changes the state of polarization of the light from linear to elliptical to circular to elliptical then linear.

Extrinsic factors result from mechanical stress due to twisting and bending of fibres or from environmental effects like temperature changes. Twisting and bending can occur during cabling process and so Polarization mode dispersion (PMD) is a strong parameter to be considered in cable design. Fibre twist creates circular birefringence whereas all the other perturbation above creates linear birefringence in which the electric field vectors of the two linearly polarized waveguide modes are aligned with the symmetry axis of the fibre.

Birefringence resulting from intrinsic and extrinsic factors may be opposite in sign and may add or subtract from each other. This causes variation of state of polarization (SOP) during light propagation. These polarization-related problems impose a two stage measurement procedure of the Brillouin gain curves. Therefore there is need to adjust the state of polarization in order to get maximum gain during the measurement. Secondly, the SOP is optimized to yield minimum, as the gain is measured [25]. The difference in phase velocities indicated by equation (3.37) is accompanied by a

difference in local group velocity and by subsequent splitting of pulses that travel through the fibre. The group velocity difference gives rise to Differential group delay(DGD), $\Delta\tau$, which is obtained by taking the derivation with respect to frequency of propagation constants of equation (3.39)[26],

$$\Delta\tau = \frac{L}{\Delta v_g} = \frac{d\Delta\beta}{d\omega} L = \left(\frac{\Delta n}{c} + \frac{\omega}{c} \frac{d\Delta n}{d\omega} \right) L \dots\dots\dots 3.40$$

3.11 Polarization Mode Dispersion

As it has been mentioned in section 3.10 above, PMD is a form of modal dispersion where two different polarization of light in a waveguide, which normally travel at the same speed, travel at different speeds due to random imperfections and asymmetries, causing random spreading of optical pulses [27]. In real optical fibres these random imperfections break the circular symmetry, thus are causing two polarizations to propagate at different speeds. In this case, the two polarization modes of a signal will slowly separate and cause pulses to spread and overlap. Because the imperfections are random, the pulse spreading effects, results in a mean polarization –dependent time differential, $\Delta\tau$ (known as the differential group delay DGD) which is proportional to the square root of propagation distance L [28].

$$\Delta\tau = D_{PMD} \sqrt{L} \dots\dots\dots (3.41)$$

D_{PMD} is the PMD parameter (coefficient) of the fibre, typically measured in ps/(km)^{1/2}. The parameter is a measure of the strength and frequency of imperfection. Single-mode optical fibres ideally are supposed to maintain a single polarization state even after long distance transmission. In practice, the optical pulse propagates along single-mode fibre in two polarization modes due to asymmetry in the fibre cross-

section [9]. The consequence of this asymmetry of cross-section is the existence of optical birefringence. As a result of birefringence, a pulse launched into the fibre at a particular state of polarization, split into two identical, linearly polarized pulses, having their electric field vectors aligned with the symmetry axes of the fibre and having different group velocities. The pulses arrive at the output differentially delayed as shown in figure 3.6. The difference in the transmission time of the two pulses polarized along the states of polarization to produce the shortest and longest propagation times is known as the Differential Group Delay (DGD) given by Eq. (3.41) which is a phenomenon that leads to pulse broadening and system impairments limiting the transmission capacity of the fibre [10, 11].

$$\Delta\tau = \left| \frac{L}{V_{gx}} - \frac{L}{V_{gy}} \right| = L|\beta_{1x} - \beta_{1y}| = L\Delta\beta_1 \dots\dots\dots 3.42$$

Where, $\Delta\tau$ is the differential group delay, L is the length of the fibre, V_{gx} and V_{gy} are the group velocities along the x and y directions and $\Delta\beta_1$ is the modal birefringence given by the difference in birefringence parameters $\Delta\beta_{1x}$ and $\Delta\beta_{1y}$.

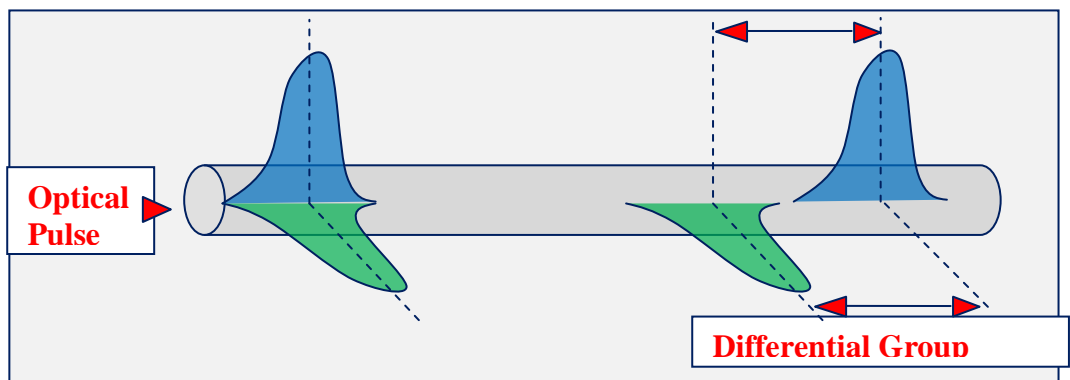


Fig 3.6 Effect of PMD in birefringence fibre on optical pulse.

An optical fibre of length z , the spectral component at a frequency ω would exit the fibre at a time delay of $T = \frac{z}{v_g}$ [29]. The group velocity v_g can be related to the phase

(propagation) constant β by:-

$$\frac{1}{v_g} = \frac{d\beta}{d\omega} \dots\dots\dots(3.43)$$

Due to the frequency dependence of phase constant, one can show that a pulse having a spectral width $\Delta\omega$ is broadened by:-

$$\Delta T = \beta_2 z \Delta\omega \dots\dots\dots(3.44)$$

Where $\beta_2 = \frac{d^2\beta}{d\omega^2}$ and is generally called the group velocity dispersion(GVD) parameter.

The GVD parameter β_2 can be interpreted as the dispersion per unit transmission distance per unit frequency spread of the signal [30]. In optical fibre communication system, the wavelength unit is more commonly used than the frequency unit and therefore equation (3.44) can be written as:

$$\Delta T = D_z \Delta\lambda \dots\dots\dots(3.45)$$

where $\Delta\lambda$ the signal spectral width in wavelength units and D_z is the dispersion parameter [31].

3.12 Polarization Effect on the Brillouin Frequency.

Since SBS originates from the coherent mixing of pump and probe waves, the efficiency is polarization dependent. Brillouin frequency resolution is one of the parameters that determine the sensors' accuracy of temperature or strain

measurement. The minimum detectable change in parameter that a sensor can detect is denoted by the equation [32].

$$\delta\nu_B, SNR = \frac{1}{\sqrt{2}} \frac{\Delta\nu_B}{(SNR)^{\frac{1}{4}}} \dots\dots\dots 3.45$$

where $\Delta\nu_B$ is full width at half maximum (FWHM). For BOTDA, $\Delta\nu_B$ represents convolution of the pulse spectrum and natural Brillouin line width, SNR is signal to noise ratio. The imperfection of the fibre core size and density non-uniformity in SMF will cause the two possible polarizations to propagate at phase velocities which are dependent on fibre locations; this is PMD [33].

From theory, the maximum Brillouin gain occurs when the pump and probe waves have identical polarization, and maximum gain is twice the minimum Brillouin gain [33]. It has been found that the output state of polarization of an arbitrary polarized input probe wave would converge to an output SOP corresponding with the maximum Brillouin gain through polarization pulling force at the high Brillouin gain condition [34]. This pulling force as well as the local birefringence of SMF govern the SOP evolution of pump and probe waves. PMD not only affects SOP of the output probe wave, but also the Brillouin frequency. From equation 3.46;

$$\delta\eta_{induced}(z) = \gamma \left| \vec{E}_{pump}(z) + \vec{E}_{probe}(z) \right|^2 \dots\dots\dots 3.46$$

where $\delta\eta_{induced}$ is the induced field, \vec{E}_{pump} is the electric field of the pump and \vec{E}_{probe} is the electric field of the probe.

It follows that the changes in SOP of the pump and probe waves are due to local changes in fibre polarization characteristics [34]. This means the Brillouin frequency

will also change along the fibre due to non-uniform density and non-circular shape variations of the fibre core. PMD introduces two error sources:

1. The change in Brillouin frequency due to birefringence change at different locations; and
2. The change in Brillouin gain due to dependence on the local SOP change of the pump and probe wave.

CHAPTER FOUR

METHODOLOGY

4.1 Introduction

This chapter presents the simulation techniques which were used to show the presence of stimulated Brillouin scattering in single mode fibre (SMF) and to determine the parameters that affect the backscattered power in SMF. Various parameters which include: - Length of fibre; Input power; PMD; Frequency and temperature were involved in the analysis. This research was done using VPI (Virtual photonics imaging) [36] simulation software.

4.2 Research Design

The setup was connected as shown in figure 4.1:-

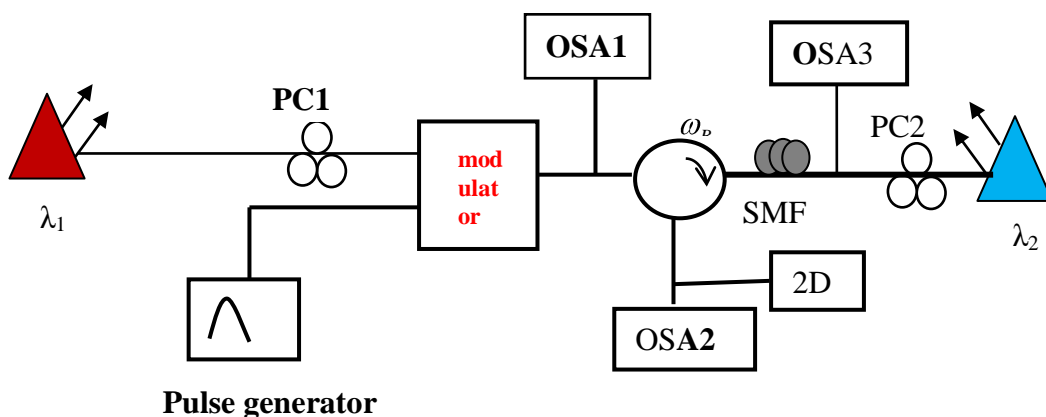


Figure 4.1 The Setup diagram used to study the existence of stimulated Brillouin scattering and parameters affecting backscattered power in optical fibre.

The set up used in the study is shown in figure 4.1 one optical fibre was used. The presence of SBS in SMF was studied using two laser sources λ_1 and λ_2 as probe and pump respectively. The probe power was set at 2 mW and the pump set at 10 mW for power amplification. The probe wave signal was pulsed at the modulator before being launched into the fibre. The circulator was used to attain bi-directional transmission over the fibre. The frequency difference between the pump and the probe was swept

in the spectral range of the Brillouin frequency shift (10.5 - 11 GHz) so that the frequency response of the fibre was determined. The backscattered spectra were recorded by Optical spectral analyzer 2 (OSA 2) while the signal power (backscattered power) was measured by the power meter and its variation with time displayed by the Two dimension (2D numerical analyzer). The probe's state of polarization (SOP) was adjusted by polarization controller PC1 while PC2 was used to maximize the pump power into the fibre. OSA1 records the input spectra OSA 3 records the transmitted spectra.

The effect of input pump power on backscattered power was studied by increasing the input power in steps of 5 dbm for a constant fibre length. The backscattered power is measured by the power meter and displayed through the numerical analyzer in each case and the spectra were also obtained from OSA2. The procedure was repeated for different fibre lengths of 20 km, 30 km, 40 km, and 50km. This is done when the frequency difference between the pump and the probe is set at about 11GHz for maximum interaction them.

As the frequency difference is set at Brillouin frequency, Simulations were done for fibre lengths of 10 km to 50 km. In each case the backscattered power was measured by the power meter. The change in backscattered power with time for the different fibre lengths was obtained from the analyzer. The frequency of the pump wave was adjusted and swept in the spectral range of Brillouin frequency shift in fibre. The backscattered power was then measured using a power meter and the results obtained from the numerical analyzer. The variation of backscattered power with time was obtained from the spectral analyzer (OSA 2). The gain as a function of position along the fibre was thus determined by the time dependence of the detected CW light. By measuring the time dependent CW signal over a wide range of frequency differences

between pump and probe, the Brillouin frequency at each fibre location was determined.

To study the effect of polarization mode dispersion (PMD) on backscattered power, the value of PMD coefficient was varied and the change in backscattered power with time was obtained from the numerical analyzer. Fibres lengths were also varied for fibres of different PMD coefficients ($0.4\text{ps}/\text{km}^2$ - $0.8\text{ps}/\text{km}^2$) and the results obtained from OSA2.

The effect of temperature on backscattered power was analyzed using the set up in figure 4.2.

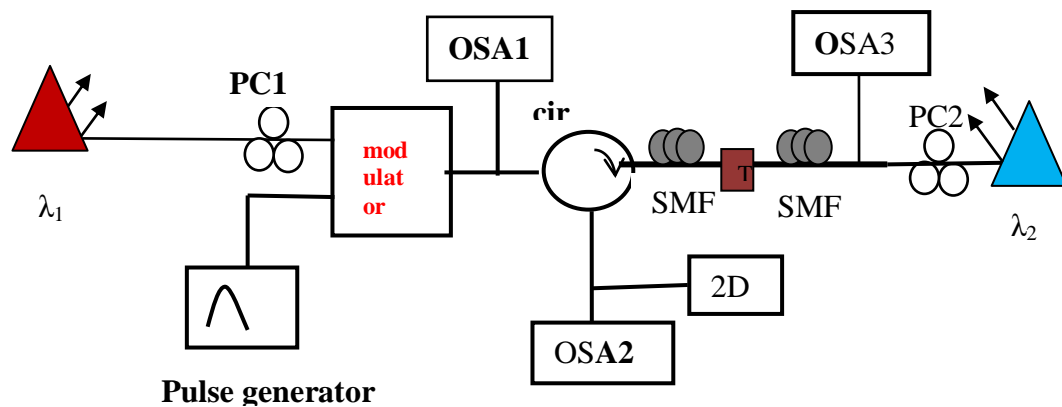


Figure 4.2 Set up for simulation on how temperature affects backscattered power

Two optical fibres were used and were connected in series. The first fibre was used as a reference and its temperature kept constant while the temperature was varied in the second fibre. The frequency difference between the pump and the probe was varied at different temperatures in the second fibre and the effect on the signal recorded from OSA2 and also from the numerical analyzer. The variation power with time for different temperatures was compared. The temperature was also swept between 200 K to 360K and the corresponding frequency shift was measured.

CHAPTER FIVE

RESULTS AND DISCUSSIONS

5.1 Introduction

In this chapter simulation results that were obtained using SMF are presented. The interaction between probe and pump wave and the SBS threshold is first shown, followed by effect of length and PMD on backscattered power and finally Brillouin frequency shift dependence on temperature.

5.2 Effect of frequency change on backscattered power.

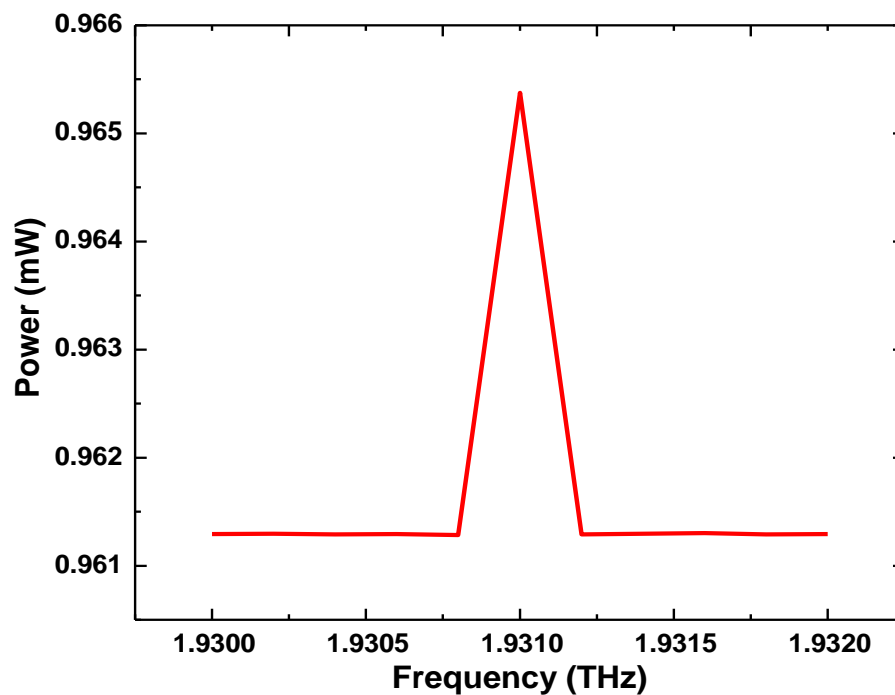


Figure 5.1 Change in signal power against change in pump frequency in a fibre.

Figure 5.1 shows that signal power increases as the frequency increases at a given frequency range until it peaks at 0.9655 mW, which correspond to a frequency of 1.9331×10^{14} Hz, which is the frequency at peak point. The power reduces again as the frequency increases by 5.0×10^{10} Hz, this is the frequency between that at peak and at the minimum power. The signal gain is a measure of optical amplification. The gain is as a result of SBS caused by interaction between acoustic waves, pump wave and

stokes wave. Since the pump and the stokes wave counter propagate in the fibre, it creates a moving interference pattern that induces acoustic wave via electrostriction effect. Thus there is transfer of energy between the pump and stokes waves that simultaneously reinforces acoustic waves. The result of this interaction is that the pump is depleted while the stoke wave is amplified as both counter propagate along the fibre. The Brillouin gain spectrum peaks at the Brillouin frequency, ν_B [15]. At frequencies below and above Brillouin frequency the backscattered power is low and constant this is due to minimal interaction between the probe wave and pump wave.

5.3 Effect of input power on Transmitted power and Backscattered power

At low input powers the backscattered power is low but increases steadily at an input of about 5dbm while the transmitted power increases and reaches saturation level for input power in excess of 10dbm.

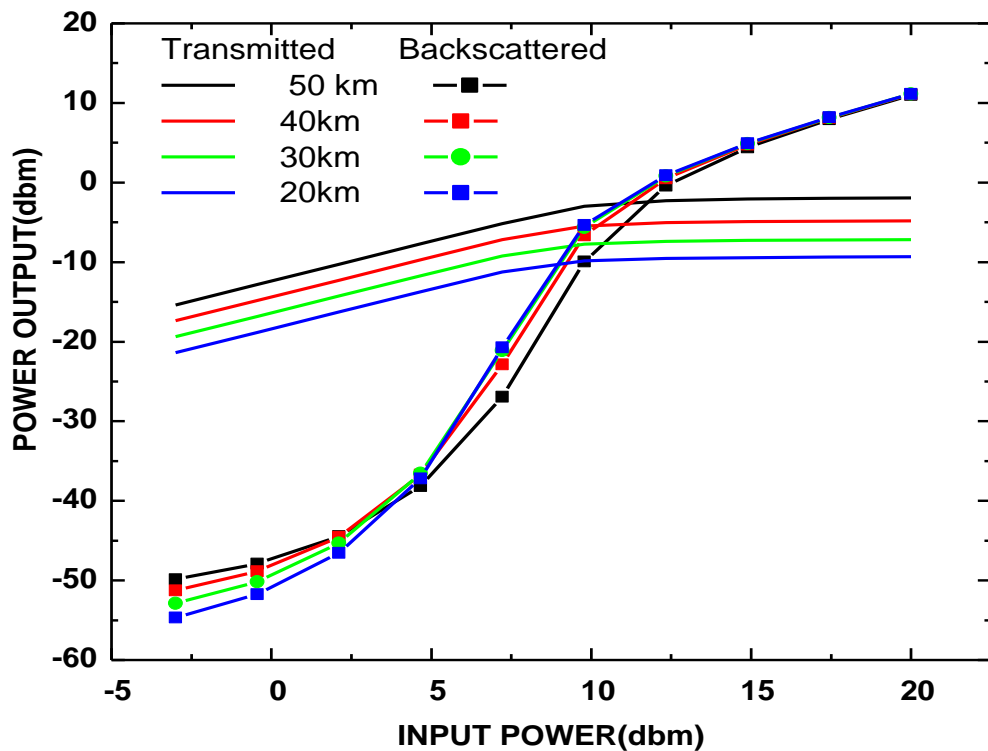


Figure 5.2 Backscattered power and Transmitted power measured as a function of the pump input power for fibres of varying lengths.

At low input powers the backscattering is dominated by simple Brillouin and Rayleigh scattering which are linear and differ from each other by Brillouin shift. But as the power is increased Brillouin scattered light is increasingly amplified by stimulation process. At 5dbm, the amount of backscattered light increases steadily with increase in input power. This is due to transfer of power to the Stokes signal via the electrostrictive process which underlies the stimulated Brillouin phenomenon. At the same time, the transmitted power at the fibre output saturates at a level that barely increases with increased input power, it becomes independent of input power. This is because at this point most of the power is backscattered.

5.4 Variation of power gain with time and length

From figure 5.3 (a) Backscattered power varies with time for various lengths the fibre. This is due to interaction of pump wave with CW probe waves as they counter propagate along the fibre resulting in optical power being transferred from the pump to probe and amplification of probe wave at points where the frequency difference between them is equal to the Brillouin frequency. SBS occurs when pump and probe overlap, resulting in an amplification of the probe wave provided that the difference between the two frequencies lies within the Brillouin gain spectrum at the overlapping position in the fibre. Backscattered Power reduces with length due to power losses along the fibre as shown in fig.5.3 (b). This is due to material absorption and scattering losses. Scattering can couple energy from guided to radiation modes, causing loss of energy from the fibre. Irregularities in core diameter and geometry or changes in fibre axis direction also cause scattering. Any process that imposes dimensional irregularities such as macro bending and micro bending increases scattering, and hence attenuation which increases with length.

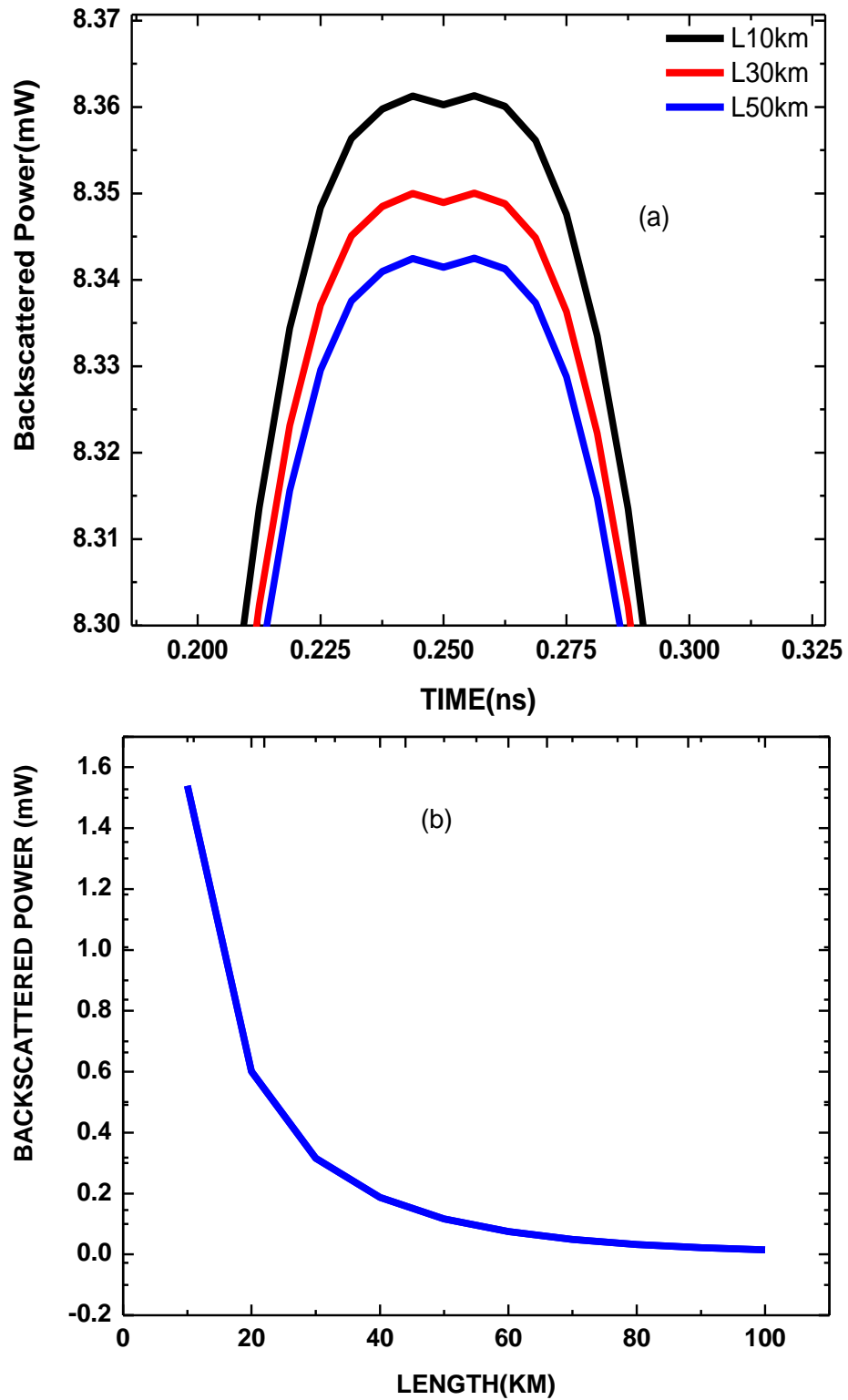


Figure 5.3(a) Variation of Backscattered power versus time for various fibre lengths
(b) Variation of backscattered power against length

5.5 Backscattered power variation with time for different SMF

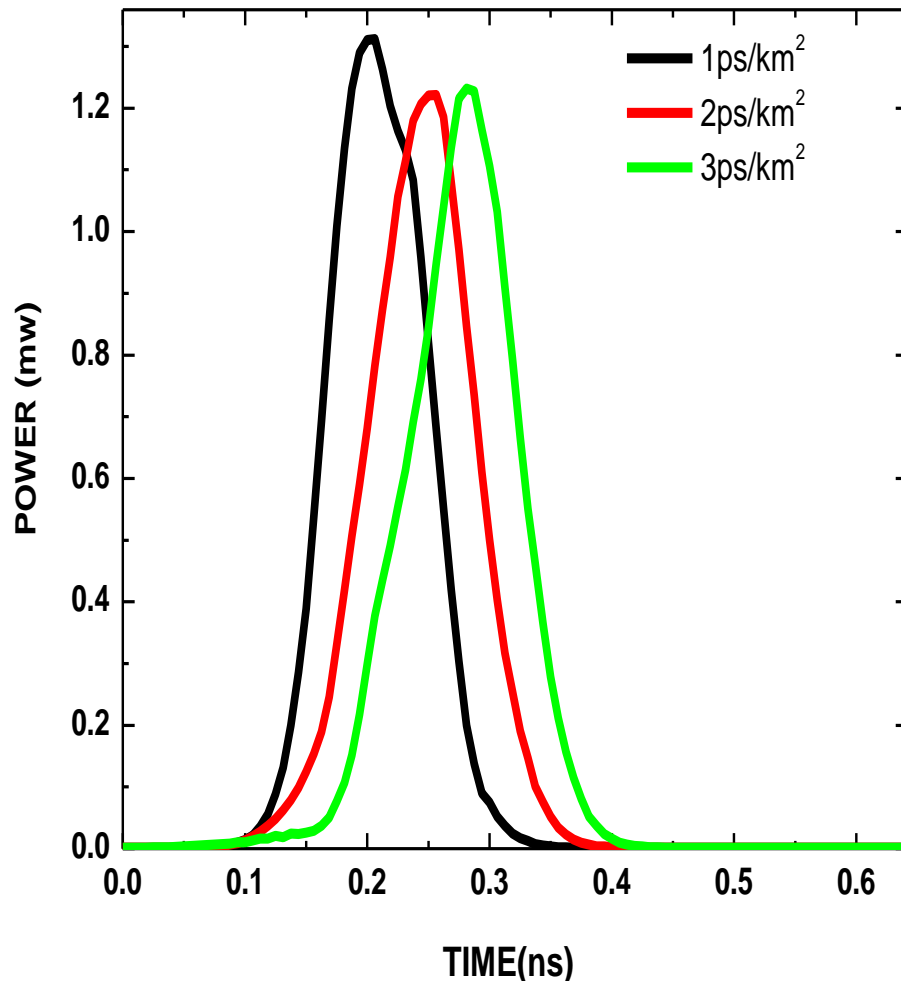


Fig.5.4 The signal power variation with time for three fibres of different PMD coefficient

Figure 5.4 shows that increase in PMD and its effect on output power over time for low PMD values. But for higher PMD values there is no much change in backscattered power. The interaction between the probe and pump ensures energy transfer from the pump to the probe signal and hence gain. However, with the introduction of PMD to the signal, this interaction is impaired. PMD causes rotation of propagation axis, which limits the probe-pump interaction and the eventual power exchange. This limitation of power transferred to the signal reduces the Brillouin gain.

5.6 Power Variation with Length for fibres with different PMD

The Figure 5.5 shows that as PMD increases, there is a remarkable increase in backscattered for fibres of length below 10km.power backscattered, but as the length increases the shift reduces. This shows that PMD affects the backscattered power as the length of the fibre increases.

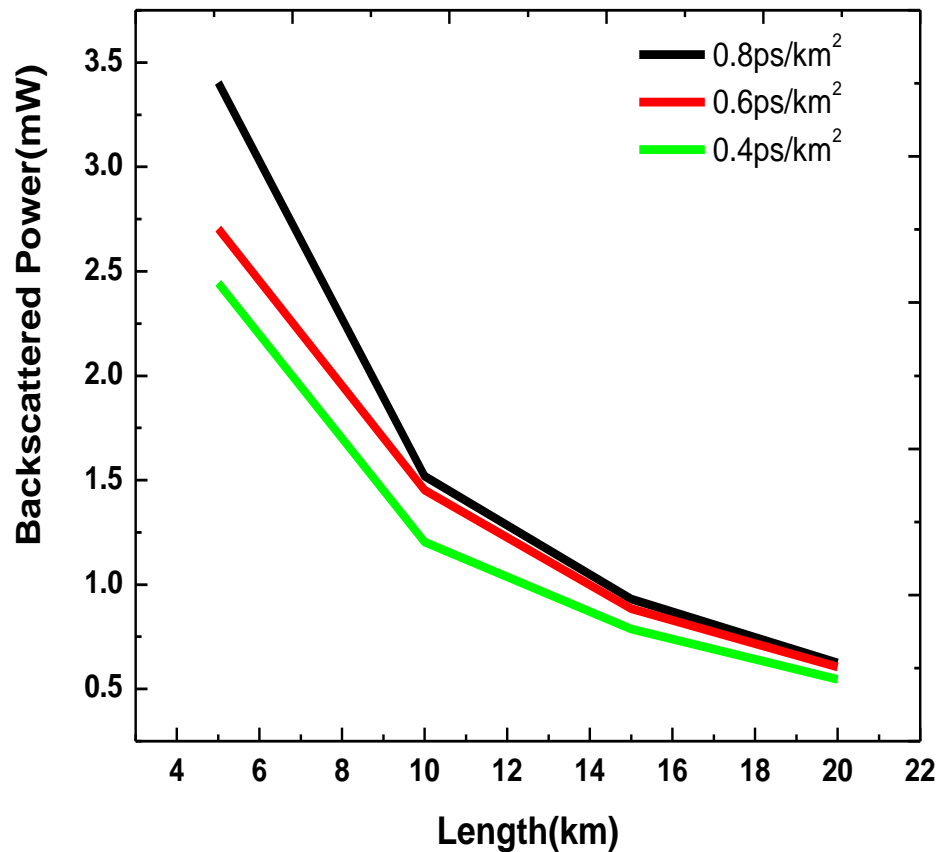


Figure 5.5 Backscattered power with change in Length for different PMD coefficients

PMD is caused by asymmetric distortions to the fibre from a perfect cylindrical geometry PMD also affects the peak Brillouin frequency due to Brillouin gain dependence from local SOP change of the pump and probe wave. Results in figure 5.6 imply that for high backscattered power a high value of PMD is preferable for fibre lengths below 10 km. However, for fibres of lengths above 15 km, there is not much variation in backscattered power for different PMD values.

5.7 Variation of backscattered power and pump frequency

Figure 5.6 shows shift in power peaks as the frequency of pump is increased. That is the maximum power changes with time for different frequencies. This is because SBS involves interaction between pump and probe waves and maximum gain was obtained when the interaction is maximum [32].

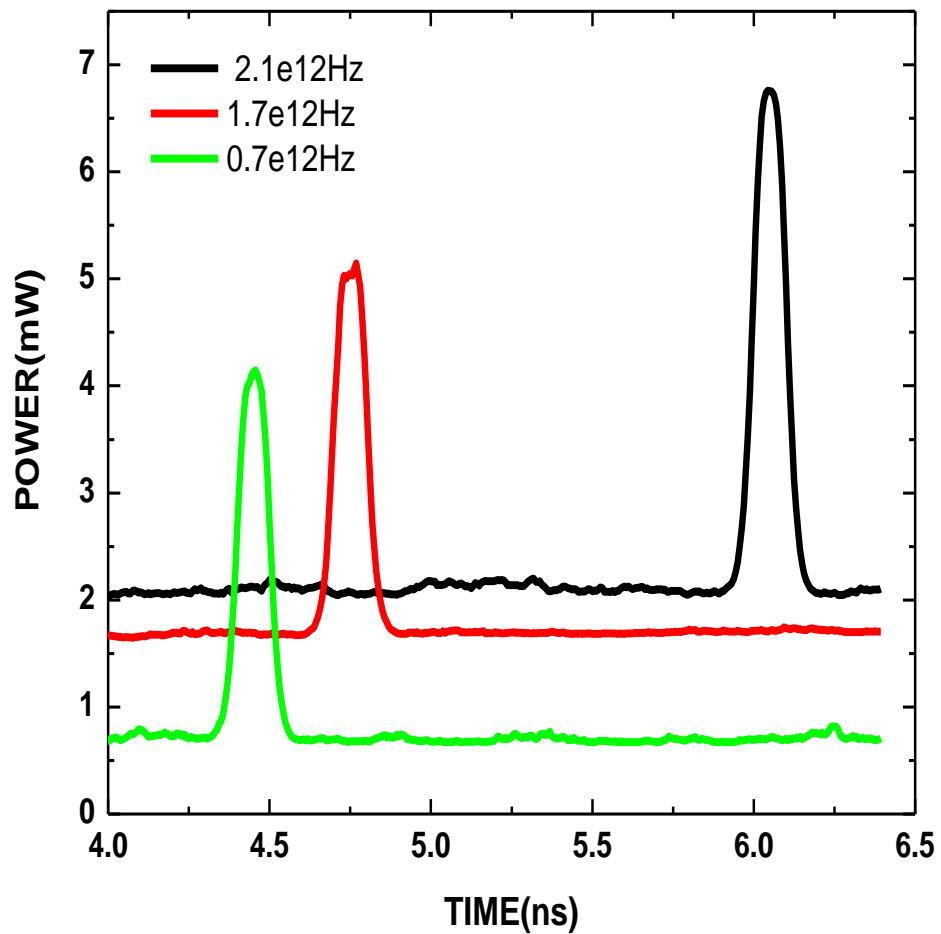
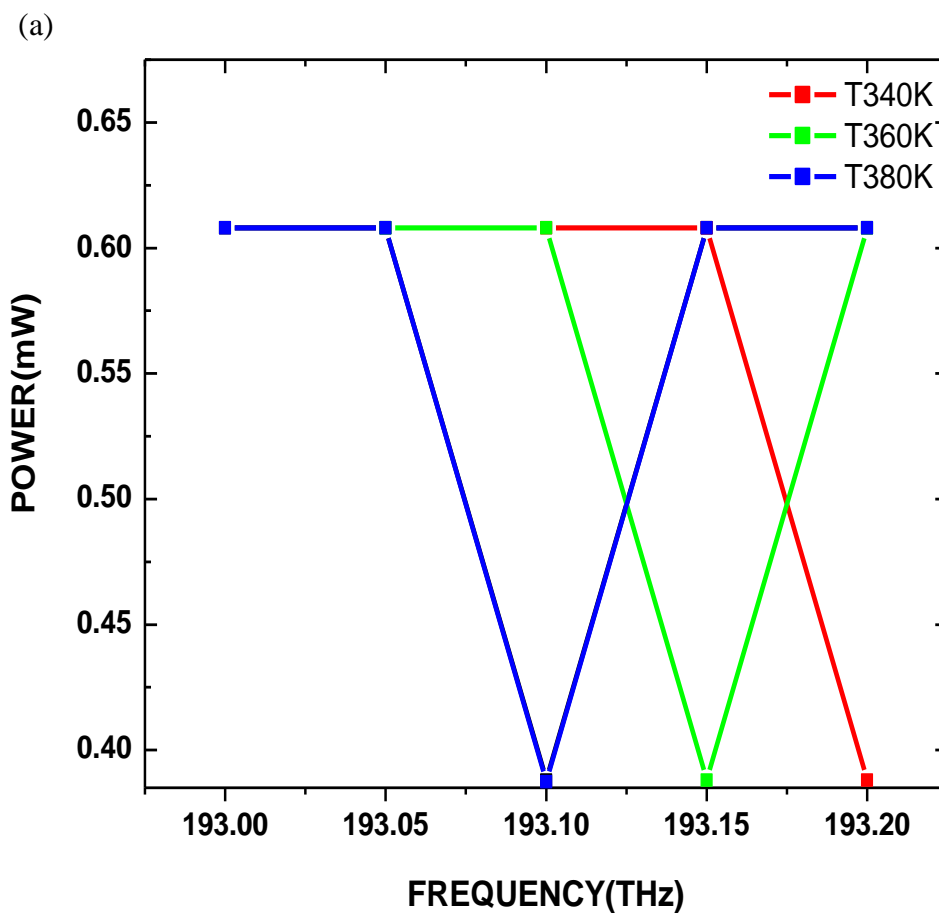


Figure 5.6 Power change against time at different pump frequencies.

5.8 Effect of frequency change on Backscattered power for different temperature and how temperature affects the frequency shift.

From figure 5.7 (a), the point of interaction between the probe and pump wave shifts with change in temperature. Temperature affects the acoustic velocity and effective refractive index of the fibre thus affecting the frequency shift and hence as the temperature changes the point of interaction changes. The Brillouin frequency shift ν_B is directly proportional to acoustic velocity, so that any change of this velocity results in a shift of the Brillouin gain spectrum. The acoustic velocity is essentially dependent on the temperature and the material density ρ_0 , so the variation of these quantities shifts the Brillouin gain spectrum.



(b)

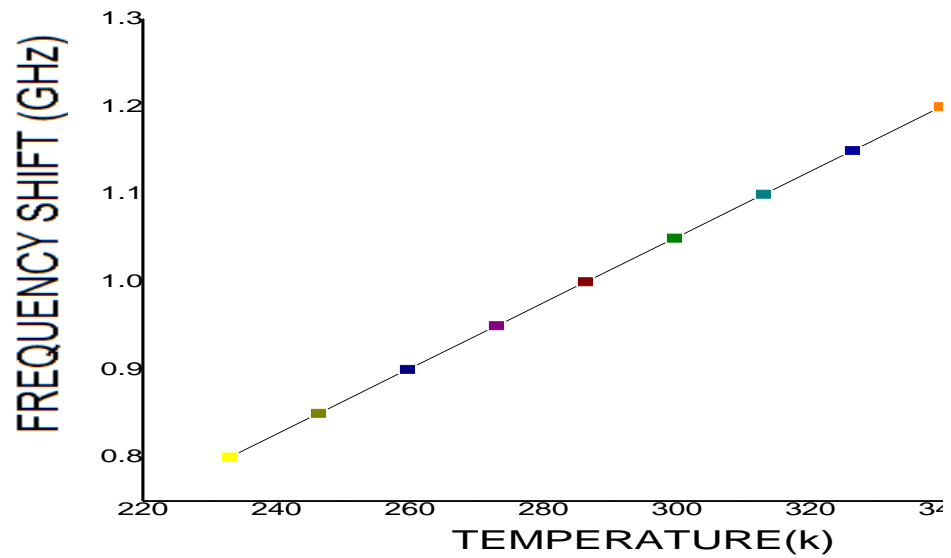


Figure 5.7 (a) Variation of signal power with frequency (b) Increase in frequency shift with temperature

5.9 Effect of temperature on power backscattered in the fibre over time.

Figure 5.8 shows the temperature profiles and the power peaks at some point along the fibre it shows that power reduces with increase in temperature.

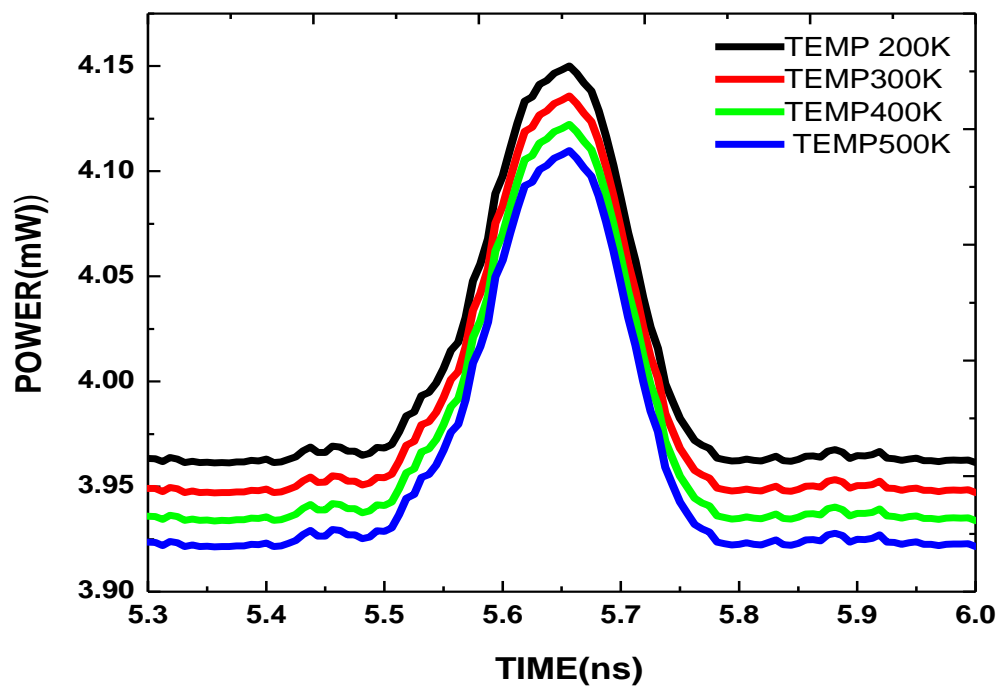


Figure 5.8 Variation in signal power with time at different temperatures.

The Brillouin gain spectrum peaks at the Brillouin frequency shift ν_B and the peak value is given by the Brillouin gain coefficient. Temperature is directly proportional to the frequency shift as from equation 3.26 and the frequency shift increases, the gain reduces. Therefore when the temperature increases, the Brillouin gain reduces.

5.10 Effect of temperature on backscattered power.

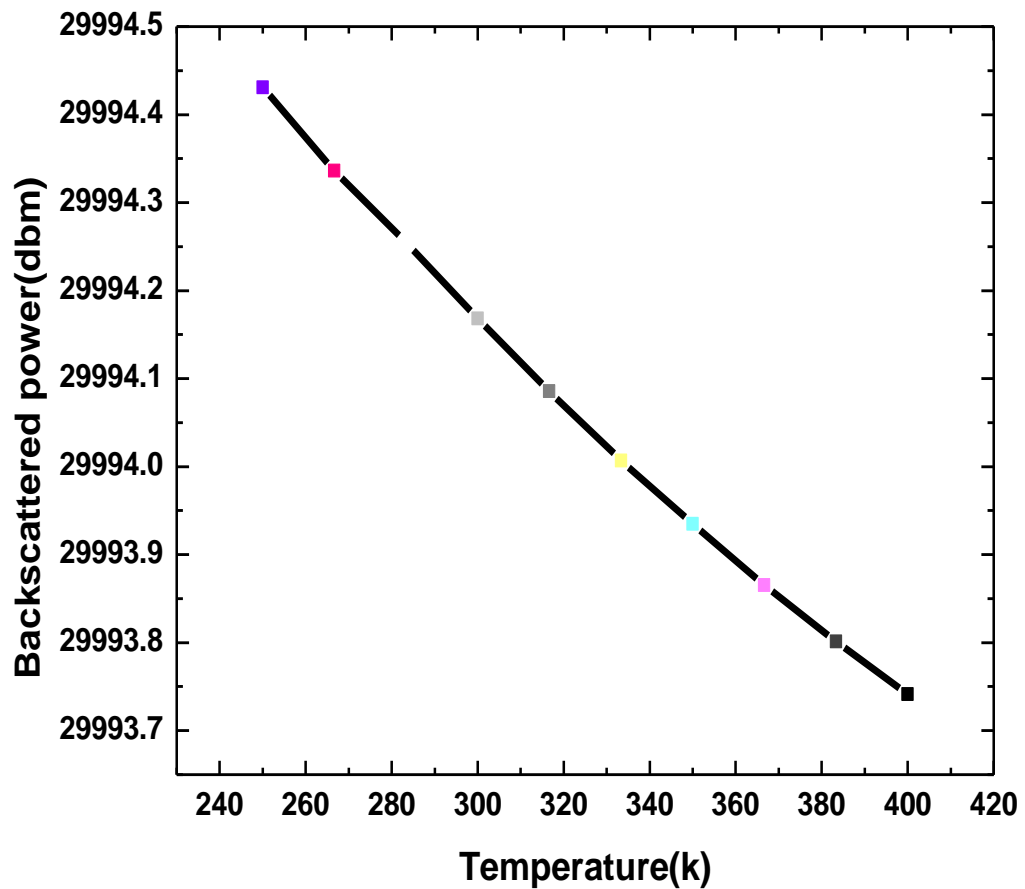


Figure 5.9 Variation of power with temperature for a fibre.

From Fig 5.9, the backscattered power is inversely proportional to temperature. Brillouin gain is inversely proportional to acoustic velocity which is directly proportional to Brillouin frequency shift. And the frequency shift increases with increase in temperature. Hence backscattered power decreases with increase in temperature.

CHAPTER SIX

CONCLUSIONS AND RECOMMENDATIONS

6.1 Conclusion

Distributed fibre optic sensor based on SBS is an attractive tool for a number of applications as outlined earlier. This work presents stimulated Brillouin scattering (SBS) process in optical fibres and the effect of various parameters on the process. For a fibre length of 25km, the SBS power threshold was found to be 5 dbm. The Brillouin gain of the optical fibre used was about $9.615 \times 10^{-4} \text{ W} \text{ _ } 9.655 \times 10^{-4} \text{ W}$ for the same fibre length. Further investigations showed that the backscattered power decreased with increase in length of single mode fibre, while polarization cause a reduction in Brillouin gain. Polarization mode dispersion in combination with SBS was found to decrease the signal power over time for low PMD values. However for higher values of PMD, there is no significant power change. The results also showed the backscattered power reduces with increase in temperature and the frequency shift is directly proportional to the temperature along the fibre. These results give a model of a sensor that is distributed and sensitive which addresses the challenges in electrical and point sensors. At the same time the detector is in the place as the power source, thus easier to operate.

6.2 Recommendation for Further Research

This study requires experimental work to validate the simulated results under various conditions.

The simulated results would be used in optimizing the effectiveness of the sensor through experimental work.

The sensor can be designed and applied particularly in monitoring of temperature/strain in large structures and landslides

REFERENCES

- [1]. Gholamzadeh, B., & Nabovati, H. (2008). 'Fibre optic sensors'. *World Academy of Science, Engineering and Technology*, 42(3), 335-340
- [2]. Bao, X., & Chen, L. (2011). 'Recent progress in optical fibre sensors based on Brillouin scattering', university of Ottawa. *Photonic Sensors*, 1(2), 102-117
- [3]. Horiguchi, T., Shimizu, K., Kurashima, T., Tateda, M., & Koyamada, Y. (1995). 'Development of a distributed sensing technique using Brillouin scattering'. *Lightwave Technology, Journal of*, 13(7), 1296-1302.
- [4]. Fellay, A. (2003). 'Extreme temperature sensing using Brillouin scattering in optical fibres'. *École Polytechnique Fédérale de Lausanne-Thèse*, (2728), 105-106
- [5]. Bernini, R., Minardo, A., & Zeni, L. (2002). 'A reconstruction technique for stimulated Brillouin scattering fibre-optic sensors for simultaneous measurement of temperature and strain'. In *Sensors, 2002. Proceedings of IEEE*, Vol. 2, pp. 1006-1011.
- [6]. Azizan, S., Shahimin, M. M., & Murad, S. A. Z. (2011, December). 'Simulation of distributed fibre optic sensor for temperature and stress sensing'. In *Humanities, Science and Engineering (CHUSER), IEEE*, pp. 449-453.
- [7]. <http://www.intechopen.com/books/fibre-optic-sensors>.
- [8]. F. Yu and S. Yin, (2002). *Fibre optic sensors*. Marcel-Dekker, (1994).
- [9]. Galindez, C. A., Madruga, F. J., Ullan, A., & Lopez-Higuera, J. M. (2009). 'Technique to develop active devices by modifying Brillouin gain spectrum'. *Electronics letters*, 45(12), pp.637-638.

- [10]. Dick, B., Gierulski, A., Marowsky, G., &Reider, G. A.(1985). ‘Determination of the nonlinear optical susceptibility $\chi(2)$ of surface layers by sum and difference frequency generation in reflection and transmission’. *Applied Physics B*, 38(2),pp 107-116 .
- [11]. Zeni, L. (2009). ‘Optical fibre distributed sensors: a tool for in-situ structural and environmental monitoring’. In *Italian Workshop on Landslides*.
- [12]. Buckland, E. L., & Boyd, R. W. (1996). ‘Electrostrictive contribution to the intensity-dependent refractive index of optical fibres’. *Optics letters*, 21(15), pp.1117-1119.
- [13]. Shen, Y. R., & Bloembergen, N.(1965). ‘Theory of stimulated Brillouin and Raman scattering’. *Physical Review*, 137(6A), A1787.
- [14]. Agrawal, G.(2010).‘Applications of nonlinear fibre optics’. Academic PressBernini, R., Minardo, A., Zeni, L., Soldovieri, F., &Crocco, L .(2004, June). ‘Distributed fibre optic Brillouin sensing in the frequency domain’. In *Second European Workshop on Optical FibreSensors*pp. 500-550.
- [15]. Nikles, M., Thevenaz, L., & Robert, P. A.(1997). ‘Brillouin gain spectrum characterization in single-mode optical fibres’. *Lightwave Technology Journal*, 15(10), 1843). International Society for Optics and Photonics. pp.1842-1851.
- [16]. Mao, X. P., Tkach, R. W., Chraplyvy, A. R., Jopson, R. M., &Derosier, R. M. (1992). ‘Stimulated Brillouin threshold dependence on fibre type and uniformity’. *Photonics Technology Letters, IEEE*, 4(1), pp.66-69.
- [17]. Boyd, R. W(2003).. *Nonlinear optics*. Academic press
- [18]. Taillaert, D., Bienstman, P.&Baets, R. (2004). ‘Compact efficient broadband grating coupler for silicon-on-insulator waveguides’. *Optics letters*, 29(23), pp.2749-2751.

- [19]. Niklès, M., Thévenaz, L. & Robert, P. A. (1996). 'Simple distributed fibre sensor based on Brillouin gain spectrum analysis'. *Optics letters*, 21(10), pp. 758-760.
- [20]. Sternklar, S.&Granot, E. E. (2003). 'Narrow spectral response of a Brillouin amplifier'. *Optics letters*, 28(12), pp.977-979.
- [21]. Minardo, A., Bernini, R., Zeni, L., Thevenaz, L.&Briffod, F.(2005). 'A reconstruction technique for long-range stimulated Brillouin scattering distributed fibre-optic sensors: experimental results'. *Measurement Science and Technology*, 16(4), pp.900 .
- [22]. Kwon, I. B., Kim, C. Y.& Choi, M. Y.(2003, August). 'Distributed strain and temperature measurement of a beam using fibre optic BOTDA sensor'. In *Proceeding of SPIE* Vol. 50, No. 57, pp. 486-496.
- [23]. Thévenaz, L., Zadok, A., Eyal, A., &Tur, M. (2008). 'All-optical polarization control through Brillouin amplification'. In *Optical Fibre communication/National Fibre Optic Engineers Conference, 2008. OFC/NFOEC 2008. Conference on*, pp. 1-3. IEEE .
- [24]. Arumugam, M.(2001). Optical fibre communication—An overview. *Pramana*, 57(5-6), pp. 849-869.
- [25]. Bao, X., Brown, A., DeMerchant, M., & Smith, J. (1999). 'Characterization of the Brillouin-loss spectrum of single-mode fibres by use of very short (< 10-ns) pulses'. *Optics letters*, 24(8), pp.510-512.
- [26]. Kyselák, M., Dorociak, P., &Filka, M.(2008). 'The Optical Modulation Format Impact on Polarization Mode Dispersion'. *International Journal of Computer Science and Network Security*, pp.27-30.

- [27]. Kondamuri, P. K. (2000). *Characterization of Polarization-Mode Dispersion on Buried Standard Single-Mode Fibres* (Doctoral dissertation, University of Kansas)
- [28]. Gordon, J. P., & Kogelnik, H. (2000). 'PMD fundamentals: Polarization mode dispersion in optical fibres'. *Proceedings of the National Academy of Sciences*, 97(9), pp.4541-4550.
- [29]. Poole, C. D., & Nagel, J. (1997). 'Polarization effects in lightwave systems'. *Optical Fibre Telecommunications IIIA*, pp. 114-161.
- [30]. Ho, K. P. (2005). *Phase-Modulated Optical Communication Systems*. Springer Science+ Business Med.
- [31]. Bao, X., Dhliwayo, J., Heron, N., Webb, D. J., & Jackson, D. A. (1995). 'Experimental and theoretical studies on a distributed temperature sensor based on Brillouin scattering'. *Lightwave Technology, Journal of*, 13(7), pp.1340-1348.
- [32]. Van Deventer, M. O., & Boot, A. J. (1994). 'Polarization properties of stimulated Brillouin scattering in single-mode fibres'. *Lightwave Technology, Journal of*, 12(4), pp. 585-590.
- [33]. Xie, S., Pang, M., Bao, X., & Chen, L. (2012). 'Polarization dependence of Brillouin linewidth and peak frequency due to fibre inhomogeneity in single mode fibre and its impact on distributed fibre Brillouin sensing'. *Optics Express*, 20(6), pp.6385-6399 .
- [34]. Virtual Photonic Imaging (VPI), <http://www.virtualphotonics.com>.

APPENDICES

Workshops and Conference Presentation

Workshop Attended

1) ALC Workshop on Lasers in Teaching and Research, 8th – 13th September, 2013.

Egerton University, Njoro.

Conference Presentation

1) E.C. Kirui, D.W. Waswa, K.M. Muguro, 'Modeling of Optical Fibre Temperature

Sensor Based On Stimulated Brillouin Scattering', Sustainable and Research Innovations (SRI) 2014 Conference (AICAD, JKUAT), 7th – 9th May 2014. Accepted.